

This is a self-archived version of an original article. This version may differ from the original in pagination and typographic details.

Author(s): Selin, Markus; Nummelin, Sami; Deleu, Jill; Ropponen, Jarmo; Viitala, Tapani; Lahtinen, Manu; Koivisto, Jari; Hirvonen, Jouni; Peltonen, Leena; Kostiainen, Mauri A.; Bimbo, Luis M.

Title: High-Generation Amphiphilic Janus-Dendrimers as Stabilizing Agents for Drug Suspensions

Year: 2018

Version: Accepted version (Final draft)

Copyright: © 2018 American Chemical Society

Rights: In Copyright

Rights url: <http://rightsstatements.org/page/InC/1.0/?language=en>

Please cite the original version:

Selin, M., Nummelin, S., Deleu, J., Ropponen, J., Viitala, T., Lahtinen, M., Koivisto, J., Hirvonen, J., Peltonen, L., Kostiainen, M. A., & Bimbo, L. M. (2018). High-Generation Amphiphilic Janus-Dendrimers as Stabilizing Agents for Drug Suspensions. *Biomacromolecules*, 19(10), 3983-3993. <https://doi.org/10.1021/acs.biomac.8b00931>

High-generation amphiphilic Janus-dendrimers as stabilizing agents for drug suspensions

Markus Selin, Sami Nummelin, Jill Deleu, Jarmo Ropponen, Tapani Viitala, Manu Lahtinen, Jari Koivisto, Jouni Hirvonen, Leena Peltonen, Mauri A. Kostianen, and Luis M. Bimbo

Biomacromolecules, **Just Accepted Manuscript** • DOI: 10.1021/acs.biomac.8b00931 • Publication Date (Web): 28 Aug 2018

Downloaded from <http://pubs.acs.org> on August 30, 2018

Just Accepted

“Just Accepted” manuscripts have been peer-reviewed and accepted for publication. They are posted online prior to technical editing, formatting for publication and author proofing. The American Chemical Society provides “Just Accepted” as a service to the research community to expedite the dissemination of scientific material as soon as possible after acceptance. “Just Accepted” manuscripts appear in full in PDF format accompanied by an HTML abstract. “Just Accepted” manuscripts have been fully peer reviewed, but should not be considered the official version of record. They are citable by the Digital Object Identifier (DOI®). “Just Accepted” is an optional service offered to authors. Therefore, the “Just Accepted” Web site may not include all articles that will be published in the journal. After a manuscript is technically edited and formatted, it will be removed from the “Just Accepted” Web site and published as an ASAP article. Note that technical editing may introduce minor changes to the manuscript text and/or graphics which could affect content, and all legal disclaimers and ethical guidelines that apply to the journal pertain. ACS cannot be held responsible for errors or consequences arising from the use of information contained in these “Just Accepted” manuscripts.

High-generation amphiphilic Janus-dendrimers as stabilizing agents for drug suspensions

Markus Selin,^{†,} Sami Nummelin,^{‡,*} Jill Deleu,^{†,§} Jarmo Ropponen,^{||} Tapani Viitala,[#]
Manu Lahtinen,[&] Jari Koivisto,[%] Jouni Hirvonen,[†] Leena Peltonen,[†] Mauri A. Kostiainen,^{‡,□}
and Luis M. Bimbo^{†,⊥,*}*

[†]Division of Pharmaceutical Chemistry and Technology, Faculty of Pharmacy, University of Helsinki, FI-00014, Finland; [‡]Biohybrid Materials, Department of Bioproducts and Biosystems, Aalto University, FI-00076, Finland; [§]Faculty of Pharmaceutical Sciences, Ghent University, 9000 Ghent, Belgium; ^{||}VTT-Technical Research Centre of Finland Ltd, P.O. Box 1000, FI-02044 VTT, Finland; [#]Division of Pharmaceutical Biosciences, Faculty of Pharmacy, University of Helsinki, FI-00014, Finland; [&]Department of Chemistry, University of Jyväskylä, FI-40014, Finland; [%]Department of Chemistry and Materials Science, Aalto University, FI-00076, Finland; [□]HYBER Center of Excellence, Department of Applied Physics, Aalto University, FI-00076, Finland; [⊥]Strathclyde Institute of Pharmacy and Biomedical Sciences, University of Strathclyde, Glasgow, G4 ORE, United Kingdom

ABSTRACT

Pharmaceutical nanosuspensions are formed when drug crystals are suspended in aqueous media in the presence of stabilizers. This technology offers a convenient way to enhance the dissolution of poorly water-soluble drug compounds. The stabilizers exert their action through electrostatic or steric interactions, however, the molecular requirements of stabilizing agents have not been studied extensively. Here, four structurally related amphiphilic Janus-dendrimers were synthesized and screened to determine the roles of different macromolecular domains on the stabilization of drug crystals. Physical interaction and nanomilling experiments have substantiated that Janus-dendrimers with fourth generation hydrophilic dendrons were superior to third generation analogues and Poloxamer 188 in stabilizing indomethacin suspensions. Contact angle and surface plasmon resonance measurements support the hypothesis that Janus-dendrimers bind to indomethacin surfaces *via* hydrophobic interactions and that the number of hydrophobic alkyl tails determines the adsorption kinetics of the Janus-dendrimers. The results showed that amphiphilic Janus-dendrimers adsorb onto drug particles, and thus can be used to provide steric stabilization against aggregation and recrystallization. The modular synthetic route for new amphiphilic Janus-dendrimers offers thus, for the first time, a versatile platform for stable general-use stabilizing agents of drug suspensions.

1. INTRODUCTION

Many newly developed active pharmaceutical ingredients (APIs) are poorly soluble in water as well as in biological fluids. Drug nanocrystals, in which the particle size of a drug is nanosized to increase its surface area, were developed to circumvent this solubility issue.¹ Media milling is currently a widely used method to reduce particle size, which in turn increases the APIs' surface area and the surface-specific drug dissolution rate. However, drug nanocrystals tend to form aggregates, or to coalesce due to the Ostwald ripening phenomenon.^{2,3} It is postulated that if a dense enough steric stabilizer layer is formed around drug particles dispersed in solution, the formation of van der Waals forces is hindered and the drug particles remain separated from each other. Hence, drug crystals must be stabilized using a polymer or a surfactant coating that increases repulsive electrostatic interactions, steric strain, and shelf-life during storage. The advantage of stabilized drug nanocrystals is that the majority of the formulated product consists of drug material, which is not easily achievable with other types of carrier-systems.⁴ Moreover, the use of stabilized nanocrystals improves drug bioavailability by other means, *e.g.*, *via* enhanced mucoadhesion and efflux inhibition.⁵ Screening methods for the production and subsequent analyses of nanosuspensions are limited,⁶ and few pharmaceutically accepted excipients are currently utilized as stabilizers.⁷ Amphiphilic copolymers, in which the different domains of the polymer have affinity towards either the adsorbent (particle surface) or dispersion medium, have been found to be suitable steric stabilizers. Among the various copolymers used for drug particle stabilization, Poloxamer 188, a non-ionic triblock copolymer composed of a hydrophobic polyoxypropylene chain edged by two hydrophilic polyoxyethylene chains, is one of the most widely used and studied.

Dendrimers are a class of well-defined, periodically branched macromolecules⁸⁻¹⁰ in which a recurrent branching of the building blocks originating from a core results in a core-shell structure.^{11,12} Intrinsic structural features of dendrimers allow for the covalent conjugation of

1
2
3 drug molecules or complexations through multivalent non-covalent interactions.^{13–15}
4 Amphiphilic Janus-dendrimers (JDs)^{16–19} are essentially synthetic surfactants, which combine
5 hydrophilic and hydrophobic dendritic domains into a single macromolecule. Their structural
6 versatility is demonstrated by the different families of JDs^{17,20–24} and Janus-
7 glycodendrimers.^{25–28} When injected from dilute organic solutions into aqueous or biological
8 media, some JDs readily self-assemble into bilayered, vesicle-like structures, *i.e.*,
9 dendrimersomes^{17,29} and glycodendrimersomes,^{30–33} or other complex architectures^{17,34,35}.
10 The shape and size of these assemblies can be controlled and even predicted using existing
11 semi-empirical models.^{36–38} Several dendrimer compositions³⁹ have been employed in diverse
12 biomedical applications,⁴⁰ *e.g.*, as a coating for 3D DNA nanostructures for improved
13 stability against endonucleases,⁴¹ as antibacterial agents with minimal eukaryotic cell
14 toxicity,⁴² as sealants for wound closure,⁴³ and as supramolecular hydrogels for sustained
15 drug release.⁴⁴

16
17
18 Here we hypothesized that high-generation amphiphilic JDs, which have a high density of
19 hydroxyl-terminated bis-MPA dendrons per molecule while at the same time exhibit
20 hydrophobic dodecyloxy chains, could be prime candidates for stabilizing colloidal drug
21 suspensions through steric stabilization. The aim of the study was to investigate if high-
22 generation JDs could be effectively used to stabilize drug suspensions of the poorly water-
23 soluble drugs indomethacin and itraconazole and compare their performance with Poloxamer
24 188. The study describes for the first time the mechanisms by which amphiphilic JDs
25 stabilize pharmaceutical drug suspensions and the influence of the number of hydrophobic
26 alkyl tails in the adsorption kinetics of the JDs to drug crystals in suspension.
27
28
29
30

2. EXPERIMENTAL SECTION

Materials.

All reagents and solvents used in the synthesis of JDs were obtained from commercial sources (Acros, Aldrich, Fisher and Rathburn; reagent grade) and were used without prior purification. Dry dichloromethane (CH_2Cl_2) and tetrahydrofuran (THF), which were used for the synthesis of intermediate compounds, were obtained from a solvent drier (MB-SPS-800, neutral alumina; MBraun, Germany) and used when necessary. The deuterated $\text{DMSO-}d_6$ for NMR analysis was purchased from Euriso-top (Saint Aubin Cedex, France). Propargyl modified bis-MPA dendrons (G1-G4) were synthesized according to Wu *et al.* (**3**, **5**, **7**, **9** Supplementary Scheme S1).⁴⁵ Percec-type hydrophobic G1 azide dendrons were prepared according to Nummelin *et al.* (**14a**, **b** Supplementary Scheme S2).^{44,46} Amphiphilic JDs 3,4-G3 and 3,4,5-G3 (Figure 1) were prepared as described previously.⁴⁴ The characterization data were in agreement with the literature. Itraconazole (Derivados Quimicos Fine Chemicals, Spain) and indomethacin (Orion Pharma, Finland) were used as model drugs. Poloxamer 188 (BASF, Germany) was used as a model stabilizer (positive control). Potassium hydroxide and acetic acid (Sigma-Aldrich, Germany) were used to make the acetic acid buffer at pH 5.00. Ethanol (99.5 %; Altia, Finland) was used as a solvent for indomethacin during the ultraviolet (UV) spectroscopy measurements. Magnesium stearate (Orion Pharma, Finland) was used as a lubricant during the tableting procedure for the contact angle measurements. Ultrapure water (18.2 M Ω .cm) was obtained from Millipore Elix 5 equipment (Merck, France).

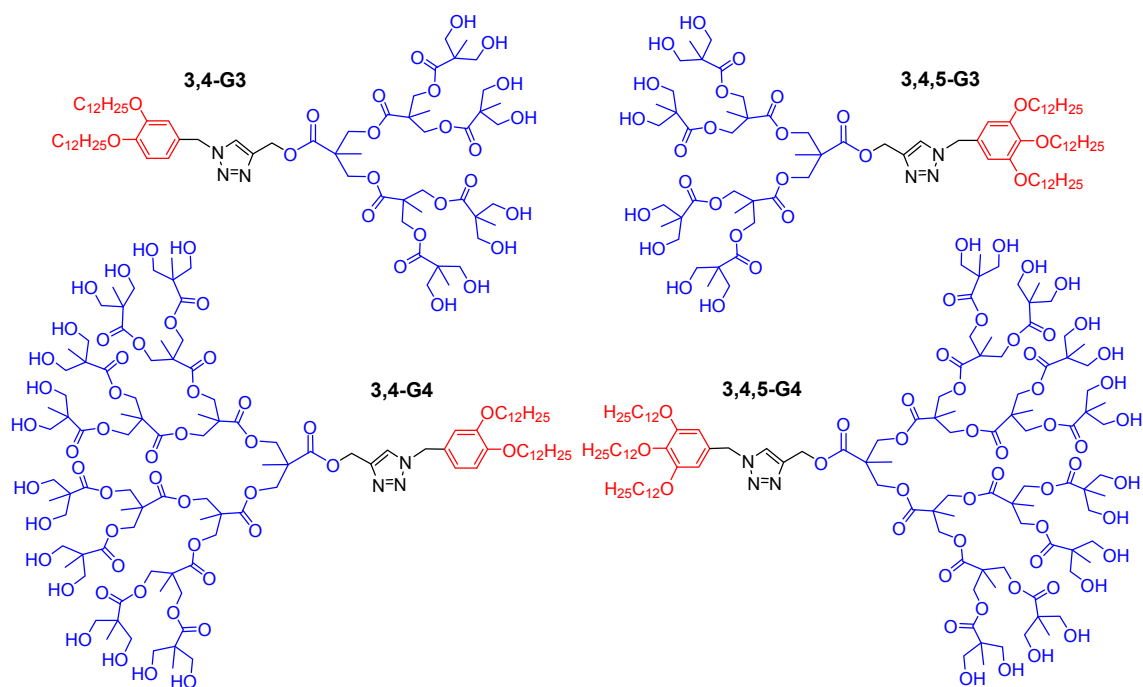


Figure 1. Chemical structures and short notation of the Janus-dendrimers evaluated in this study.

Synthesis and characterization of Janus-dendrimers.

General Procedure. The azide dendron **14a** or **14b** (1.05 eq.), G3 or G4 bis-MPA-alkyne **7** or **9** (1 eq.), and sodium L-ascorbate (20 mol %) were dissolved in THF in a vial. Cu(II)SO₄ (10 mol %) was dissolved in H₂O and added to the reaction. The mixture was stirred for 5 min at RT before DMSO was added. The mixture was stirred 24 h at 60 °C before it was cooled to RT. The crude product was purified by flash chromatography on SiO₂, affording Janus-dendrimers as off-white solids (see Supporting Information Schemes S1-S4 for details).

Nuclear Magnetic Resonance (NMR). ¹H NMR (400 MHz) spectra and uniform driven equilibrium Fourier transform (UDEFT, pulse program: *udeft*) ¹³C NMR (100 MHz) spectra were recorded on a Bruker Avance DPX400 spectrometer equipped with a 5 mm BBFO probehead. Chemical shifts (δ) were reported in ppm (Figures S1-S4). The residual protic

1
2
3 solvent of DMSO- d_6 (^1H , δ 2.50 ppm; ^{13}C , δ 39.50 ppm) was used as the internal reference.
4
5 Coupling constants (J) were reported in Hertz (Hz). Heteronuclear ^1H - ^{13}C connectivities were
6
7 determined by adiabatic HSQC experiments (pulse program: *hsqcetgpsisp.2*).
8

9 **Matrix-assisted Laser Desorption/Ionization Time-of-Flight Mass Spectrometry**
10 **(MALDI-TOF)**. The analyses were carried out using a Bruker UltrafleXtreme MALDI-
11
12 TOF/TOF mass spectrometer (Bruker Daltonics, Bremen, Germany) equipped with a
13
14 SmartBeam II laser (355 nm) operating at 2 kHz with a 200 μm raster in reflectron positive
15
16 mode. FlexAnalysis v3.4 was used to assign molecular isotopic masses in the 200-4000 Da
17
18 mass range. 2,5-Dihydroxybenzoic acid (DHB) mixed in a THF (10 mg mL^{-1}) was used as a
19
20 matrix. A concentration of 2 mg mL^{-1} of the sample in THF was mixed with the matrix
21
22 solutions in 1:1 (v:v) ratio and applied to the stainless steel target plate. Sample droplets were
23
24 dried under a gentle air stream at room temperature to obtain small crystals that simplified
25
26 ionization. A peptide calibration standard II (Bruker starter kit # 8208241) was used for
27
28 calibration.
29
30
31
32

33 Thermal analysis.

34 For each JD, a physical mixture with bulk indomethacin was prepared by weighing and
35
36 mixing 20.0 mg of the bulk drug and 2.0 mg of a solid dendrimer, respectively. The resulting
37
38 mixtures, as well as neat JDs and indomethacin, were then subjected to thermal analysis.
39
40 Thermal transitions were measured using a Mettler Toledo 823e (Switzerland) differential
41
42 scanning calorimeter and were processed using STARE software (Mettler Toledo, version
43
44 9.00). Samples (3–7 mg) were annealed for 5 min at 25 $^{\circ}\text{C}$ before they were heated to 190 $^{\circ}\text{C}$
45
46 at 10 $^{\circ}\text{C min}^{-1}$ heating rate. Nitrogen was used as a purge gas at a 50- mL min^{-1} flow rate.
47
48 Thermal transitions as peak maximas ($^{\circ}\text{C}$) and enthalpies (kcal mol^{-1}) are reported in
49
50 Supporting Information Tables S2 and S3. Indium was used as a calibration standard both for
51
52 temperature and enthalpy. Melting points for the 3,4-G4 and 3,4,5-G4 JDs were taken as the
53
54 maxima of the endothermic peaks.
55
56
57
58
59
60

Contact angle.

Aqueous dendrimer solutions (0.4 mg mL^{-1}), an aqueous poloxamer solution (1.0 mg mL^{-1}), and water were used for the contact angle measurements. The contact angles were measured on cylindrical drug compacts produced from 300 mg bulk indomethacin in an infrared spectroscopy pellet ($\varnothing 13 \text{ mm}$) by applying one-ton compression for 10 s using an Atlas 15.001 manual hydraulic press (SPECAC, England). A sample solution droplet (ca. 2 μL) was deposited onto an indomethacin compact, and images were captured once per second for 1 min using a Cam200 Contact Angle Meter (KSV Instruments, Finland) and were processed using Attension Theta software (Biolin Scientific, version 4.1.0). The average and standard deviation of the contact angles are presented as functions of time.

Surface plasmon resonance.

The interactions of indomethacin with 3,4-G4, 3,4,5-G4, and the poloxamer reference were determined by surface plasmon resonance (SPR) measurements performed using a 4-channel multi-parametric MP-SPR 200 instrument (BioNavis, Finland) equipped with a 670-nm laser and a peristaltic pump (Ismatec, Germany). Indomethacin was deposited onto gold SPR sensor surfaces from aliquots of a saturated indomethacin solution that was pre-prepared by shaking indomethacin in ethanol (4 mg mL^{-1}) overnight. The SPR signal baseline was first recorded in pure water, and the SPR sensograms were obtained by recording the change in the SPR angle approximately every 5.3 s during 50 μM aqueous stabilizer solution injection for 15 min (association phase) and subsequently during pure water injection for at least an additional 15 min (dissociation phase). For comparison, the SPR measurements were repeated with plain gold sensors alone. The recorded data were baseline corrected using the background data and were modelled using Matlab R2014a software (MathWorks, version 8.3.0.532) with an in-house algorithm that removes measurement disturbances with a simple input method and optimizes the range of time points to fit the exponential decay models to the association and dissociation phases.

Manual milling.

Bulk indomethacin or itraconazole (4.0 mg) were placed in a glass test tube with 3.0 g of zirconium oxide beads (\varnothing 1 mm), and 1 mL of the aqueous stabilizer solution was used as the milling medium. The tube was capped, and the bulk drug was manually milled utilizing vortex-mixing: 60 s continuous milling periods and 15 s pauses were alternated until the total milling time reached 6 min. Longer manual milling times were not required for the screening, as it has been shown that the rate of particle size reduction decreases during extended milling periods.⁶

Particle preparation.

The indomethacin suspensions were manually milled in aqueous dendrimer solutions (0.40 mg mL⁻¹) and were stored at RT. An aqueous poloxamer solution (1.00 mg mL⁻¹) was used as the milling medium for the positive controls, and water without excipients was used as the milling medium for the negative controls. In order to separate any JD aggregates from the drug particles, all four JD solutions were also subjected to a manual milling process without indomethacin and were monitored in parallel with the indomethacin suspensions.

Particle sizing.

Particle size was measured using dynamic light scattering (DLS). The milled drug suspensions were vortex-mixed for 30 s, diluted 40-fold with water, and briefly mixed again prior to subjecting the dilutions to the DLS analysis in a disposable plastic cuvette. Z-average size and PDI were recorded. DLS analyses were performed at 25 °C using a Zetasizer[®] Nano ZS (Malvern Instruments, UK) equipped with 4 mW He-Ne laser 633 nm and an avalanche photodiode positioned at 173° to the beam. Instrument parameters and measurement times were determined automatically. The size was determined based on an average of 12 measurement runs in triplicate.

Stability studies.

After milling, the suspensions were subjected to particle size analysis for four weeks. During the first week, the repeatability of the milling process was followed with three

1
2
3 separately milled samples. From the second to the fourth week, the particle size of a single
4
5 sample was monitored weekly.
6

7 Re-dispersion studies.

8 For the re-dispersion studies, two separately milled suspensions were pooled, and 700 μL
9
10 of the suspension was dried on well plates in an oven for 4 d at 40 $^{\circ}\text{C}$. Saturated aqueous
11
12 indomethacin solutions were subsequently prepared and filtered. The dried samples were
13
14 dispersed in 700 μL aliquots of the saturated indomethacin solutions, followed by 3 min of
15
16 sonication (35 kHz) prior to subjecting the re-dispersed suspensions to particle size analysis.
17
18

19 UV spectrophotometry.

20 The UV absorption spectra of 40 $\mu\text{g mL}^{-1}$ indomethacin in ethanol and 100 $\mu\text{g mL}^{-1}$ 3,4-G4
21
22 in water (Figure S5) were recorded from 190 nm to 400 nm using a quartz cuvette and a UV-
23
24 1600PC spectrophotometer (VWR international, China) to select wavelengths for subsequent
25
26 UV determinations. At 318.5 nm, indomethacin has a local absorbance maximum and the
27
28 absorbance of the dendrimer is at minimum. Therefore, this wavelength was selected for the
29
30 determination of indomethacin content in solutions with the dendrimers. Accordingly, the
31
32 indomethacin content in the milled suspensions was determined as follows: 10 μL of each
33
34 suspension was dissolved in 990 μL of ethanol, and then the indomethacin content of the
35
36 solutions was determined using a calibration curve (318.5 nm wavelength). The drug content
37
38 in each suspension was calculated based on triplicate measurements.
39
40
41

42 At 260.3 nm, indomethacin has high absorbance values, and the dendrimer has a local
43
44 absorption minimum, whereas at 280.0 nm, the absorbance of indomethacin is reduced, and
45
46 the dendrimer has a local absorption maximum. Monitoring absorbance at 260.3 nm allows
47
48 for the estimation of indomethacin content that is below the lower limit of detection at 318.5
49
50 nm. In such a case, the influence of the dendrimer concentration on the results should be
51
52 monitored based on the absorbance values at 280.0 nm. Finally, neither indomethacin nor the
53
54 dendrimer absorb light at a 400 nm wavelength. In theory, light scattering due to particulate
55
56
57
58
59
60

1
2
3 matter in the samples can distort the UV determinations. Thus, the absorbance of each sample
4
5 was also measured at a 400.0 nm wavelength.
6

7 Saturation solubility.

8 Bulk indomethacin (10.0 mg) was weighed into glass vessels, and 1.5 mL of a 12 mM
9 acetate buffer (pH 5.0) was added to the vessels. Next, 0.5 mL of aqueous dendrimer solution
10 (0.4 mg mL⁻¹), aqueous poloxamer solution (1.0 mg mL⁻¹), or water was added. The vessel
11 was sealed tightly, placed for overhead shaking in a REAX 2 shaker (Heidolph, Germany) for
12 24 h at RT, and allowed to stand for 12 h before the solution was filtered through a 0.2 μm
13 filter. The absorbance of the filtered solution was determined at four pre-defined
14 wavelengths. The indomethacin content was determined using a UV spectroscopy calibration
15 curve (260.3 nm). The concentration of indomethacin in the saturated solution, as well as the
16 absorbance at 280.0 nm were recorded.
17
18
19
20
21
22
23
24
25
26
27

28 Dissolution rate.

29 Dissolution experiments were conducted with 500 mL of a 12 mM acetate buffer (pH 5.0)
30 stirred (50 rpm) using a DT6 dissolution apparatus (Erweka, Germany) in an ET 15001
31 (Erweka, Germany) heat bath at 37 °C. Independently milled indomethacin suspensions were
32 stored at RT for 1 d before subjecting them to the dissolution experiment. Each measurement
33 with the suspensions began with placing 500 μL of a vortex-mixed suspension into the
34 dissolution chamber of the apparatus. The dissolution experiments with bulk indomethacin
35 began with measuring 2.0 mg of non-milled indomethacin powder into the dissolution vessel
36 and pouring 500 mL of a pre-warmed, 12 mM acetate buffer (pH 5.0) into the vessel at the
37 start of the experiment. The dissolution process was monitored as a function of time by taking
38 1 mL aliquots from the dissolution media at defined time points. The indomethacin content in
39 the samples was determined using a UV spectroscopy calibration curve (318.5 nm). The
40 extent of dissolution was calculated for the dissolution samples at each time point, and the
41 averages and standard deviations of the dissolution profiles were calculated and reported.
42
43
44
45
46
47
48
49
50
51
52
53
54
55
56
57
58
59
60

3. RESULTS AND DISCUSSION

Screening study design.

To validate the manual milling methodology for the screening studies, indomethacin was media-milled in an aqueous Poloxamer 188 solution (positive control) and in water (negative control). For the manual milling method, the initial Z-average size was 1231 nm for the positive control and 814 nm for the negative control. The positive control was selected on the basis of earlier studies: when indomethacin is mechanically milled using poloxamer as the stabilizer, monodisperse submicron drug particles are obtained.⁴⁷ The presence of poloxamer in the samples should not influence the DLS results by changing the viscosity of the dispersant, as a 2000-fold concentration increase only changes the viscosity of the aqueous solution to 1.26 mPas⁴⁸ from *ca.* 0.89 mPas (the viscosity of plain water at RT). Therefore, the difference in the initial sizes of the controls should reflect a successful adsorption of poloxamer onto the indomethacin particles or a slightly reduced milling efficiency. After three weeks of storage at RT, the Z-average size of the positive control only showed a moderate increase (+121 nm) compared to the negative control (+3667 nm). Small-scale manual milling reduced the size of the particles in indomethacin suspensions, and the suspensions were successfully stabilized by the poloxamer (positive control). Hence, it was concluded that this experimental approach could be used in screening studies involving JDs.

A preliminary screening of JDs with two different drugs (indomethacin and itraconazole) was conducted to confirm their particle size stabilizing efficiency and the proper concentration of dendrimer solutions, as well as to select the model drug for further investigations. Three different concentrations of 3,4-G4 were used in the screenings, as follows: low (0.04 mg mL⁻¹), medium (0.10 mg mL⁻¹) and high (0.40 mg mL⁻¹). Additionally, poloxamer was also investigated as a stabilizer for both indomethacin and itraconazole at a concentration of 1.0 mg mL⁻¹ to provide a benchmark for the JDs. Manually milled indomethacin and itraconazole suspensions were stored at 4 °C for 138 and 144 days,

1
2
3 respectively. After four months of storage, all the suspensions were subjected to particle size
4 analysis and, as a conclusion, indomethacin suspensions showed smaller *Z*-average size and
5 narrower size distribution than itraconazole suspensions, and poloxamer-stabilized
6 suspensions (Figure S6). The observed low reproducibility of this screening method,
7 especially in the case of itraconazole, is assumed to be due to the manual milling procedure
8 and the hardness of the drug compound. Mechanization of the process, together with longer
9 milling times, is expected to decrease the variability of the results. The conservation of the
10 smaller *Z*-average for extended periods of time is one of the hallmarks of successful drug
11 particle stabilization.⁵ Poloxamer was found to prevent agglomeration during the four month
12 storage, and under our experimental conditions the JDs performed equally or better with only
13 a fraction of the concentration required for poloxamer. This is thought to be due to the high
14 density of hydroxyl terminated bis-MPA dendrons per molecule which leads to a strong
15 physical barrier on the particles' surface that hinders the attractive van der Waals' forces
16 between particles. Furthermore, the mechanical milling procedure of bulk indomethacin
17 required less time and material in contrast to bulk itraconazole, which required at least two
18 grams of material.⁴⁹ Therefore, indomethacin was selected as the sole model drug to be
19 further studied with the four different types of JDs, namely G3 and G4 both with 3,4- and
20 3,4,5-branching (Table S1). The data collected from the preliminary screenings led us to
21 choose a 1:10 dendrimer-to-drug mass-ratio for preparing the forthcoming indomethacin
22 suspensions by manual milling.
23
24
25
26
27
28
29
30
31
32
33
34
35
36
37
38
39
40
41
42
43
44
45
46
47
48

49 Interaction studies.

50 The thermal behavior of the pristine JDs and the JD-indomethacin physical mixtures (JD:IND
51 = 1:10) were analyzed using differential scanning calorimetry (DSC) to discern physical
52 interactions and the chemical compatibility of the mixtures. All dendrimers, except 3,4-G3,
53 displayed a broad melting transition ($> 6 \text{ kcal mol}^{-1}$) preceded by one or two weaker
54
55
56
57
58
59
60

1
2
3 endothermic transitions (Figure 2, Table S2), which most likely indicate a small-scale
4 structural re-arrangement (solid-state phase transition) of the dendritic branches. The 3,4,5-
5 branched JDs generally showed about 20 °C higher melting points than their 3,4-branched
6 analogues. In the case of 3,4-G3, due to its amorphous nature, a glass transition ($\Delta C_p = 0.08$
7 kcal mol⁻¹ K⁻¹) was observed at 94.3 °C accompanied with a structural relaxation (enthalpic)
8 peak on top of it. Moreover, 3,4,5-G3, and 3,4,5-G4 dendrimers exhibited liquid crystal
9 phases, as weak endothermic isotropization transitions were observed in the DSC curves at
10 169.8 and 152.8 °C, respectively. Neat indomethacin showed only a sharp melting transition
11 (T_m) at 160.4 °C ($T_e = 159.3$ °C), which corresponds with the melting temperature of the
12 crystalline γ -form of indomethacin.⁵⁰

13
14 Physical mixtures of the JDs and indomethacin systematically exhibited the same
15 endothermic transitions corresponding with those previously observed for their individual
16 components, as evidenced by the DSC curves (Figure 2 and Table S3). Generally, the
17 endotherms of the dendrimer components become somewhat more difficult to observe in the
18 scans as the weight fraction of the JDs, and consequently, the magnitude of transitions,
19 became only 1:10 that of pristine JDs. Nonetheless, only the isotropization peak of the LC
20 phase of 3,4,5-G4 (152.8 °C) was missing in the DSC curve, but was likely buried underneath
21 the broadened indomethacin melting peak and thus not evident. Predictably, the melting
22 transitions of indomethacin showed somewhat broader melting ranges and small downward
23 shifts in peak maxima (1.0-1.5 °C). This phenomenon is caused by the well-known “impurity
24 effect”, which occurs when small amounts of a foreign substance are added to a pure
25 component, and it is commonly reported for physical mixtures of stabilized drugs as well. For
26 example, the shift from 165.0 °C to 133.6 °C (50:50) and 112.3 °C (30:70) has been reported
27 for indomethacin and poloxamer mixtures.⁵¹ In conclusion, the absence of major
28 discrepancies in the thermal events confirms that JDs and indomethacin do not show eutectic
29
30
31
32
33
34
35
36
37
38
39
40
41
42
43
44
45
46
47
48
49
50
51
52
53
54
55
56
57
58
59
60

melting behavior, co-crystal formation, or induction of polymorphs because indomethacin remains in crystalline γ -form. In addition, the overall crystallinity of the JD-indomethacin mixtures remained unchanged after mixing.

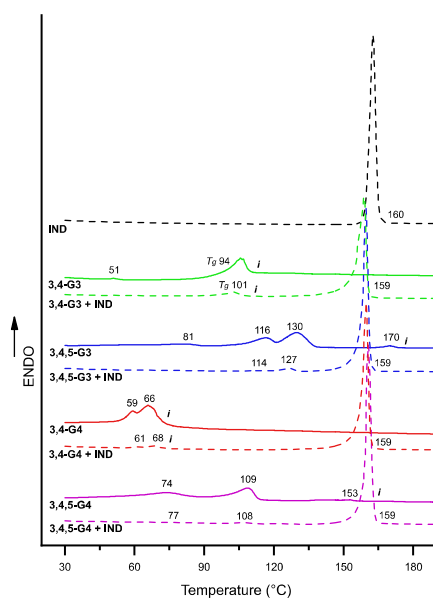


Figure 2. DSC curves [$10\text{ }^{\circ}\text{C min}^{-1}$] of Janus dendrimers (colored solid line), indomethacin (black dashed line, and physical mixtures of Janus dendrimers (10 wt.%) and indomethacin (colored dashed line). Transition temperatures are marked in each curve as peak maxima [$^{\circ}\text{C}$].

As discussed by Bakatselou *et al.*,⁵² surfactants may promote the wetting of drug particles, thereby increasing the drug dissolution rate. Therefore, contact angle measurements of aqueous solution droplets on compressed indomethacin surfaces were carried out to investigate the wettability of the drug when in contact with different JDs and the poloxamer (Figure 3). The procedure mimics the media milling conditions in which solid drug particles are dispersed in aqueous stabilizer solutions. The measured contact angles of water and the aqueous poloxamer solution were in agreement with the literature data.⁴⁷ The contact angles measured between the dendrimer solutions and indomethacin were consistently higher than

1
2
3 the contact angles between poloxamer solution and indomethacin. In general, the contact
4
5 angles between aqueous dendrimer solutions and indomethacin were comparable to the
6
7 contact angle values between plain water and indomethacin at the end of the experiment. In
8
9 contrast, the contact angle between the 3,4-G3 solution and indomethacin was slightly lower
10
11 than the contact angle between water and indomethacin. A careful examination of the contact
12
13 angles as a function of time revealed that the contact angles of samples that contained 3,4-G3
14
15 and 3,4-G4 JDs decreased faster than the contact angle values between water and
16
17 indomethacin. The contact angles of 3,4,5-G3 and 3,4,5-G4 followed the contact angle values
18
19 between water and indomethacin throughout all experiments. Studies investigating
20
21 hydrocarbon materials have suggested that contact angles between liquids and coated solid
22
23 materials reflect the properties of the solvent-exposed chemical groups of the coatings rather
24
25 than those of the bulk solid.^{53,54} Accordingly, if a drop of an aqueous solution of a stabilizer
26
27 has a lower contact angle on the indomethacin surface than a drop of water, a decrease in the
28
29 contact angle value due to the presence of dissolved stabilizers should reflect reductions in
30
31 the solid-liquid and liquid-vapor interfacial energies caused by the adsorption of the materials
32
33 onto these interfaces. As the dendrimers with fewer aliphatic chains in the hydrophobic
34
35 dendron (3,4-G3 and 3,4-G4, as opposed to 3,4,5-G3 and 3,4,5-G4) displayed some surface-
36
37 active characteristics under these experimental conditions, it is assumed that these dendrimers
38
39 enable drug particle wetting to a greater extent which could aid the dissolution process.
40
41 However, none of the dendrimers achieved the same reduction in contact angle as the
42
43 poloxamer.
44
45
46
47
48
49
50
51
52
53
54
55
56
57
58
59
60

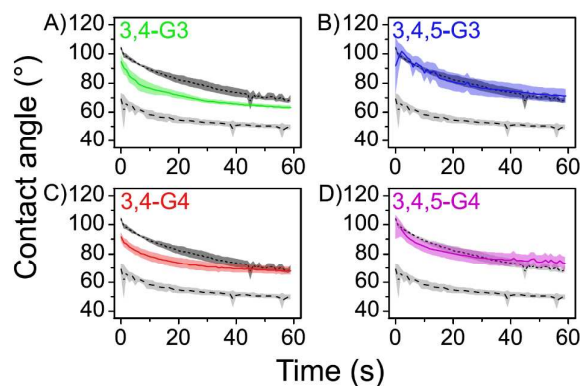


Figure 3. Contact angle of a drop of aqueous **A)** 3,4-G3, **B)** 3,4,5-G3, **C)** 3,4-G4, and **D)** 3,4,5-G4 solution (0.4 mg mL^{-1} deposited onto an indomethacin tablet; solid line \pm colored area), aqueous poloxamer solution (1.0 mg mL^{-1} ; line with long dashes \pm light gray area) and water (line with short dashes \pm dark gray area). Chemical structures are abbreviated with colored text. The solid line curves are the average of three separate measurements \pm standard deviation, represented as the colored area.

The interactions between the drug and dendrimers were further studied using MP-SPR to identify the solid-liquid interface interactions independent of the interactions at the liquid-air and solid-air interfaces. In general, G4 JDs and poloxamer adsorbed onto plain gold (Figures 4A–C) and indomethacin surfaces (Figures 4D–F). The injection of G3 JDs did not result in detectable changes in the SPR peak angular positions (data not shown). The G4 JDs showed very little or no desorption from plain gold or indomethacin surfaces (Figures 4A–B and 4D–E), whereas poloxamer clearly desorbed from the surfaces (Figures 4C and 4F). Because the SPR peak angular position values were above the baseline levels at the end of the poloxamer desorption process, it was concluded that the desorbed fraction of the poloxamer molecules were incompletely attached to the surfaces or were only entangled with other poloxamer molecules. The dendrimers did not desorb from the surfaces, which indicates that a steady state SPR peak angular position in the adsorption phase was reached due to surface

1
2
3 saturation. For each sample, the adsorption onto the indomethacin surface was slower than
4
5 onto the plain gold surface. Moreover, the poloxamer sample was the fastest and the 3,4,5-G4
6
7 sample the slowest to reach steady state values during SPR responses (Figure S7). Changes in
8
9 SPR responses arise when the molecules in the aqueous phase are adsorbed onto the sensor
10
11 and cause refractive index changes near the surface. In detail, the binding events are
12
13 converted to a change in the measurable sensor output value at efficiency, which depends on
14
15 the recognition element and the analyzed compound. Therefore, the magnitude of the SPR
16
17 responses should not be directly compared between chemically distinct samples; however, as
18
19 the 3,4,5-G4 has a structure related to 3,4-G4 and also showed slower adsorption kinetics
20
21 than 3,4-G4, it is postulated that the bulkier hydrophilic side sterically hinders the packing of
22
23 3,4,5-G4 on the surfaces. The ideal features of a steric stabilizer in terms of steric hindrance
24
25 rely on the affinity of the stabilizer to the particle surface as well as to the dispersant.⁷ In
26
27 addition, polymeric steric stabilization does not usually destroy the crystal structure of drug
28
29 particles, unlike the action of conventional small molecular weight surfactants e.g. sodium
30
31 dodecyl sulfate (SDS). The irreversible adsorption of the JDs to the indomethacin surfaces
32
33 corroborates the hypothesis that the stabilization of drug particles occurs mainly due to steric
34
35 hindrance and not by decrease of the surface tension in which little to no adsorption would
36
37 take place.
38
39
40
41
42
43
44
45
46
47
48
49
50
51
52
53
54
55
56
57
58
59
60

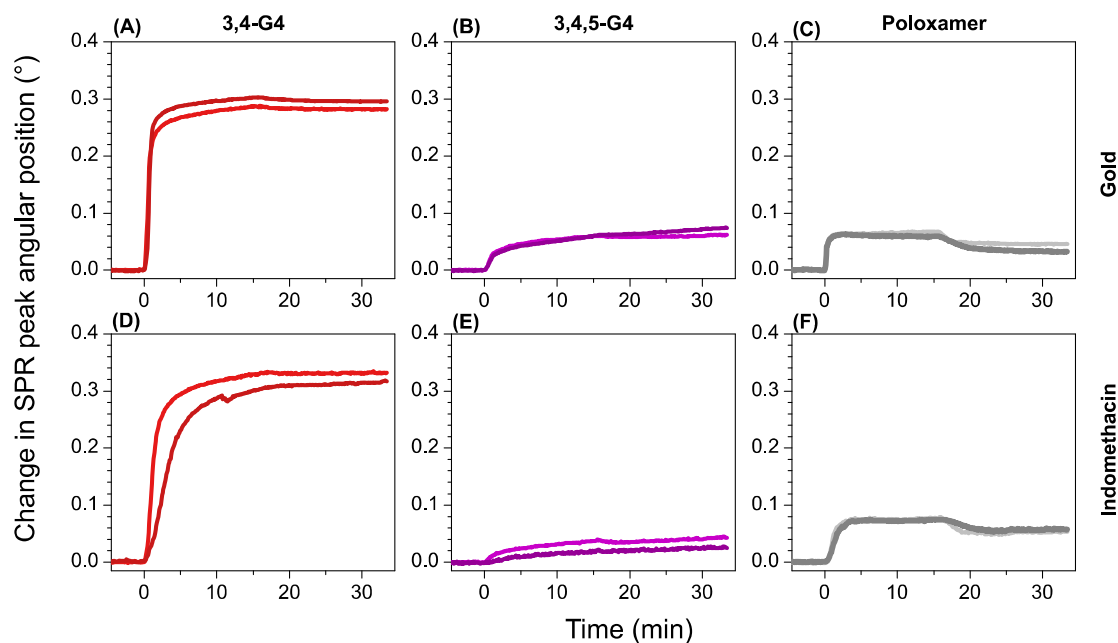


Figure 4. The SPR angle data for 3,4-G4 (A and D), 3,4,5-G4 (B and E), and poloxamer (C and F) for measurements conducted on pure gold (A–C) and indomethacin covered (D–F) SPR sensors. The association phases (the first 15 min) preceded the dissociation phases (from 15 to 33.4 min). The two different curves in each panel are repeated measurements of the same system.

Particle size stabilization.

Next, the particle size reduction and the stabilization of the indomethacin suspensions were screened in the presence of dendrimers using DLS. Four and seven days after milling, the Z-average size of the suspension milled in the presence of 3,4-G3 showed the largest Z-average size values (8549 ± 2853 nm and 9346 ± 2481 nm, respectively), which is a clear indication of aggregation. The Z-average sizes of the suspensions with 3,4,5-G3 (2228 ± 631 nm and 2334 ± 161 nm), 3,4-G4 (1084 ± 128 nm and 1561 ± 659 nm) and 3,4,5-G4 (1983 ± 475 nm and 1937 ± 352 nm) were noticeably smaller and mostly non-aggregated.

Indomethacin suspensions in aqueous dendrimer solutions (samples) and dendrimers solutions alone (background controls) were milled and monitored weekly over a four-week

1
2
3 period (Figures 5 and S8) to examine the stability of the coated drug particles. In general, the
4
5 samples showed larger Z-average sizes than the background controls. Considering this and
6
7 the ratios of the sample components, the Z-average sizes of the samples should mainly reflect
8
9 the Z-average size of the indomethacin crystals in the suspensions. A closer examination of
10
11 the results from indomethacin milled in the presence of 3,4-G3 revealed that during the four-
12
13 week period the measured Z-average sizes showed large variations (3049 nm) and
14
15 considerably irregular developments (Figure 5A). In contrast, the Z-average size of the
16
17 indomethacin suspensions milled with 3,4,5-G3, 3,4-G4 and 3,4,5-G4 (Figures 5B–D) varied
18
19 less over the four-week period, increasing 690 nm, 283 nm, and 259 nm, respectively. For
20
21 3,4,5-G3, the comparatively high uniformity and abundance of small JDs' background
22
23 structures in the control measurements (Figure S8) raised a question regarding the potential
24
25 bias in the stability results, which is discussed later in the text. Structure-activity comparisons
26
27 between the dendrimers with the 3,4-hydrophobic dendron (3,4-G3 and 3,4-G4) suggested
28
29 that the G4 hydrophilic dendron is required for particle stabilization. In conclusion, the 3,4-
30
31 G3 showed the weakest performance as a stabilizer, whereas repeatable and stable
32
33 indomethacin particles were obtained in the presence of G4 JDs. The results demonstrate the
34
35 potential of G4 JDs to stabilize drugs in submicron suspensions at low dendrimer-to-drug
36
37 mass ratios.
38
39
40
41

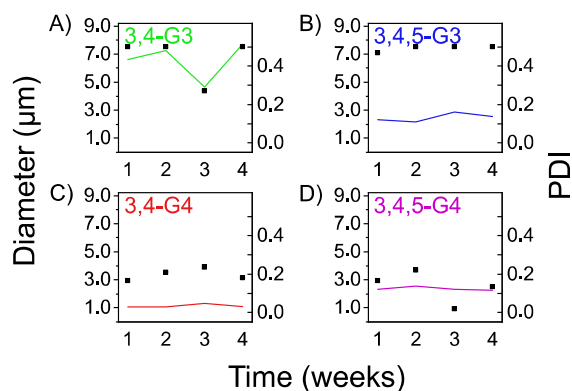


Figure 5. Development of the Z-average size (left axis, line) and PDI (right axis, squares) of an aqueous **A**) 3,4-G3, **B**) 3,4,5-G3, **C**) 3,4-G4, and **D**) 3,4,5-G4 solutions milled with indomethacin. Chemical structures abbreviated with colored text.

Suspensions obtained through media milling are often formulated as dry dosage forms. To obtain dosage forms with enhanced dissolution behaviors, the reduced size of the particles should be maintained through downstream processing, dry storage, and subsequent re-dispersion. To study the stabilizing performance of the dendrimers in this context, the milled indomethacin suspensions were dried, and the particle sizes were determined after re-dispersion (Figure 6). In the presence of the dendrimers and poloxamer, the indomethacin particles had a Z-average size ranging from *ca.* 1 to 4 μm after drying and re-dispersion. In the absence of these materials, indomethacin particles had a Z-average size of *ca.* 27 μm . The best stabilizing performances were observed for G4 JDs. It should also be noted that the dry state stabilizing performances of the G3 JDs were as good as the stabilizing performance of the poloxamer.

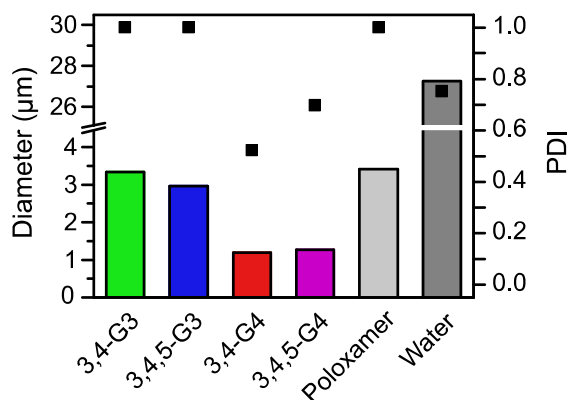


Figure 6. Z-average size (left axis, colored area) and PDI (right axis, black squares) after drying and re-dispersion of indomethacin suspensions milled in the presence sample materials (n=1).

Saturation solubility.

To examine the solubilizing potential of the dendrimers, solubilized indomethacin contents were determined from aqueous solutions saturated with an excess of the bulk drug (Table 1). The apparent solubility of indomethacin was moderately increased in buffer solutions supplemented with the dendrimers compared to the solubility in plain buffer. The absorbance values of 3,4-G4 containing saturation solubility samples at a 280-nm wavelength were *ca.* 2 % of the values expected based on the UV spectrum recorded from the 3,4-G4 (Figure S5). This could indicate that a majority of the dendrimers was adsorbed onto non-dissolved, bulk drug particles and then removed during filtration. Considering the absorbance values of the other samples at 280 nm, the same held true for the other dendrimers, including 3,4,5-G3 which formed background nanostructures in aqueous solutions. The formation of background structures was not considered when interpreting the results of the contact angle measurements. The formation of self-associated nanostructures might compete against 3,4,5-G3 adsorption on the surfaces of an aqueous drop thereby reducing the ability of the dendrimer to influence the contact angle. However, the lack of dissolved 3,4,5-G3 in the saturation solubility experiment supported the initial interpretations of the contact angle data, and contradicted the existence of the self-associated background structures in the milled indomethacin suspensions stabilized with 3,4,5-G3, thereby confirming the particle size stabilizing potential of the JDs.

Table 1. Solubility of indomethacin and absorbance at 280.0 nm as measured in 2 mL of 9 mM acetate buffer (pH 5.0) supplemented with indomethacin and the solubilizing agents (n=1).

Solubilizing agent		UV spectroscopy results	
Janus-dendrimer	Content	Indomethacin solubility	Absorbance

or control	[mg mL ⁻¹]	[μg L ⁻¹]	[AAU]
3,4-G3	0.30	590.1	0.0175
3,4,5-G3	0.30	434.3	0.0104
3,4-G4	0.30	493.5	0.0134
3,4,5-G4	0.30	557.2	0.0170
Poloxamer	0.75	541.8	0.0121
None	N/A	401.4	0.0107

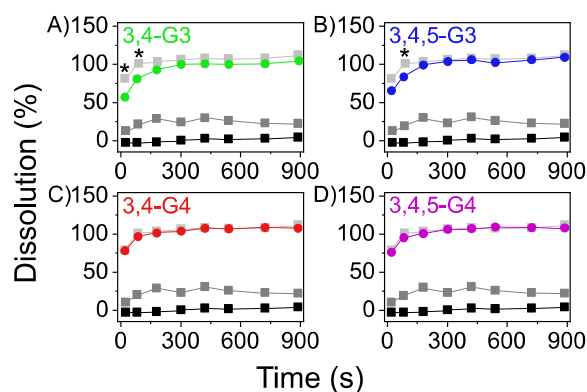
Abbreviations: not applicable (N/A), arbitrary absorbance unit (AAU)

The solubility of indomethacin in a plain pH 5.0 buffer was one order of magnitude lower than a value reported in the literature⁵⁵ but well in-line with indomethacin solubility in acidified water at RT,⁵⁶ however, water solubility over one order of magnitude higher (16 mg L⁻¹) has also been suggested for indomethacin.⁴⁸ The variations in the values reported in the literature might reflect the pH sensitivity of the solubility determinations close to the pK_a value of indomethacin (4.3),⁵⁷ the temperature dependence of indomethacin solubility,⁵⁸ the differences in the dissolution characteristics of indomethacin polymorphs,⁵⁹ and the effects of the experimental methodologies.⁶⁰

Dissolution rate.

The dissolution of indomethacin reached 90 % of the indomethacin contents within 3 min in all samples milled in the presence of dendrimers and poloxamer (Figure 7A–D), and the extent of dissolution in these samples did not decrease over the measured period. In contrast, the dissolution of indomethacin milled in water reached only 30 % of the indomethacin content within 3 min and decreased to 22 % at the end of the experiment. For further comparison, bulk indomethacin (non-milled drug powder) reached 4 % dissolution within the time frame of the experiment. The extent of bulk indomethacin dissolution agreed with the extent of dissolution expected at an equilibrium state (roughly 10 %). Conversely, the

1
2
3 maximum extent of dissolution observed for the negative control in the dissolution
4
5 experiment (30 %) greatly exceeded the measured saturation solubility.
6
7



8
9
10
11
12
13
14
15
16
17
18
19
20
21
22 **Figure 7.** Dissolution results of A) 3,4-G3, B) 3,4,5-G3, C) 3,4-G4, and D) 3,4,5-G4 samples
23 (colored circles), the poloxamer control (light grey squares), negative control (grey squares \pm
24 gray area) and bulk drug (black squares) as measured at 318.5 nm wavelength ($n = 3$). The
25 asterisk represents significant differences between the sample and the poloxamer control ($p =$
26 0.05). Chemical structures abbreviated with colored text.
27
28
29
30
31
32
33

34 The dissolution of indomethacin (Figure 7) co-occurred with the disappearance of drug
35 particles scattering light (Figure S9). Scattering was not evident in the results of
36 indomethacin milled without any stabilizer or bulk indomethacin. For the remainder of the
37 milled indomethacin suspensions, the recorded absorbance values at 400 nm were small and
38 sloped downward during the first three minutes of the experiment. This indicates that light
39 scattering can be detected using this method and that scattering should only slightly affect the
40 intensity of the light transmitted through the samples at the beginning of the experiment when
41 a large number of particles is present and a majority of the drug has not yet dissolved. In
42 general, the results indicate that milling enhances the dissolution of indomethacin and that the
43 dendrimers can stabilize the indomethacin suspensions produced by milling.
44
45
46
47
48
49
50
51
52
53
54
55
56
57
58
59
60

1
2
3 The samples milled in the presence of 3,4-G3 and 3,4,5-G3 (Figure 7A–B) showed slightly
4 slower dissolution rates compared to the poloxamer control, whereas the samples milled in
5 the presence of 3,4-G4 and 3,4,5-G4 (Figure 7C–D) showed dissolution rates comparable to
6 the poloxamer control. It is noteworthy that indomethacin particles stabilized with 3,4,5-G3
7 and 3,4,5-G4 had comparable Z-average sizes, but the particles stabilized with 3,4,5-G4
8 reached 90 % dissolution faster than the particles stabilized with 3,4,5-G3. As both JDs have
9 3,4,5-substituted hydrophobic dendrons and there might be a bias in the 3,4,5-G3 size results,
10 only a speculative structure-activity comparison of the hydrophilic dendrons is given at this
11 stage. The 3,4,5-G3 has less hydrogen bond donors and acceptors than 3,4,5-G4, which might
12 lead to slower kinetics in the coating desorption and a simultaneous decrease in the
13 dissolution of indomethacin. The average extent of indomethacin dissolution in the samples
14 containing 3,4-G3 did not reach as high percentage values as the samples containing the other
15 dendrimers (Figure 7). Also, the particles persisted longer in the 3,4-G3-containing samples
16 than in the poloxamer control and the samples stabilized with the other dendrimers (Figure
17 S9). In order to maintain a steric barrier that is able to minimize inter-particle interactions to a
18 level that the attractive van der Waals forces are lower than the repulsive steric forces, the
19 stabilizing moiety needs to be sufficiently long and dense.³ The less dense hydroxyl-
20 terminated bis-MPA dendron of the G3 JDs is therefore less efficient in promoting steric
21 stabilization as the G4 JDs, which have double the hydroxyl-terminated bis-MPA groups.
22 Therefore, a higher Z-average size and polydispersity is observed for G3-stabilized drug
23 particles compared to the G4-stabilized ones (Figure 5), as well as a lower efficiency in
24 promoting drug dissolution (Figure 7).
25
26
27
28
29
30
31
32
33
34
35
36
37
38
39
40
41
42
43
44
45
46
47
48
49

50 Solubility enhancement.

51 The reduction of particle size during the media milling process increases the total surface
52 area of indomethacin and improves the rate of dissolution according to the Noyes-Whitney
53 equation. Moreover, size reduction has also been shown to increase the surface specific
54
55
56
57
58
59
60

1
2
3 dissolution rate.⁶¹ The suggested mechanism relies on interpreting the combined effect of the
4
5 particle size's dependent terms according to the Prandtl boundary layer equation for flat
6
7 surfaces (Equation S1), *viz.* dissolving boundary layer length (L) and the velocity of the
8
9 solvent in relation to the dissolving surface (V), as the correlated reduction of the
10
11 hydrodynamic boundary layer thickness (h_H) and the distance of molecular diffusion in the
12
13 dissolution process. According to Keck and Müller⁶², saturation solubility increases as the
14
15 equilibrium between dissolution and recrystallization shifts due to increasing dissolution
16
17 rates. Therefore, the enhanced solubility of indomethacin in the negative control of the
18
19 dissolution experiment is the result of size reduction (Figure 6). For the other samples in the
20
21 dissolution experiment the observed enhancement of solubility may be due to the combined
22
23 effect of the size reduction and the presence of solubilizing and wetting agents.^{52,58} As
24
25 previously noted, the contact angles between aqueous dendrimer solutions and indomethacin
26
27 surfaces were relatively high, which indicates that the dendrimers do not influence the
28
29 wetting of indomethacin. Moreover, assuming a constant ratio between the amounts of the
30
31 solubilizing agent and the increments in the solubilized indomethacin content (Table 1), the
32
33 size reduction seems to largely dictate the extent of solubility enhancement.
34
35
36

37
38 Enhanced solubility is maintained in the stabilized indomethacin suspensions with broad
39
40 particle size distributions, especially in samples containing 3,4-G3 (Figures 5A and 7A). This
41
42 may be explained by applying a polymeric net crystal growth inhibition model, which relies
43
44 on the Kelvin equation, to the dendrimer coated drug crystals in the suspensions.⁶³ In essence,
45
46 even a partial coverage of the seed crystal surfaces is enough to inhibit crystal growth.
47
48 According to the rationale presented, the size reduction also enhances the dissolution rate of
49
50 the dendritic coatings on size-reduced particles with high surface curvatures. Hence, while
51
52 the coatings and the drug molecules of the small particles dissolve rapidly, the coatings of the
53
54 larger particles should persist longer and should slow the recrystallization of indomethacin.
55
56
57
58
59
60

1
2
3 An apparent lack of recrystallization might also be caused by the slow kinetics of
4 indomethacin recrystallization,⁶⁴ however, the slow indomethacin recrystallization in the
5 stabilized samples reflects a shortage of non-coated seed crystal facets in the dissolution
6 media, as the extent of dissolution sloped downward in the negative control but not in the
7 stabilized suspensions during the dissolution experiment.
8
9
10
11
12

13 14 15 4. CONCLUSIONS

16 High generation amphiphilic JDs (G3 and G4) obtained *via* a copper catalyzed click-
17 chemistry reaction using a modular synthesis approach were used to screen submicron drug
18 crystal stabilization. The screening methodology applied minimizes the use of stabilizing
19 materials, and the results demonstrate a good applicability of the G4 JDs as stabilizers in
20 media milling and the subsequent dry-state processing of pharmaceuticals. The dense steric
21 layer induced by the hydroxyl terminated bis-MPA dendrons in the G4 JDs plays a critical
22 role in the stabilization process preventing the drug particles' agglomeration for extended
23 periods of time, while enabling low polydispersity values when compared with G3 JDs and
24 Poloxamer 188. Further, the SPR measurements support the hypothesis that JDs irreversibly
25 adsorb onto the indomethacin surfaces *via* hydrophobic interactions and that the number of
26 hydrophobic alkyl tails determine the adsorption kinetics of the JDs. In addition, both G4 JDs
27 increase the drug dissolution rate of poorly water soluble compounds to the same extent as
28 the poloxamer at a lower stabilizer-to-drug ratio. We thus believe that the modular synthesis
29 approach for JDs described here offers a convenient and efficient route for the stabilization of
30 poorly water-soluble drugs in suspension. As a result, we envisage that these structures may
31 be further tailored and scaled-up for pharmaceutical processing purposes.
32
33
34
35
36
37
38
39
40
41
42
43
44
45
46
47
48
49
50

51 52 53 ASSOCIATED CONTENT

54 55 **Supporting Information.**

1
2
3 The Supporting Information is available free of charge on the ACS Publications website at
4
5 DOI:

6
7 Synthesis details (Scheme S1-S4), ^1H -NMR and ^{13}C -NMR spectra (Figures S1 and S3),
8
9 adiabatic HSQC 2D NMR spectra (Figures S2 and S4), UV spectra (Figure S5), sample usage
10
11 (Table S1), preliminary screening results (Figure S6), thermal transitions and enthalpies
12
13 (Table S2 and S3), average rate parameter values and magnitude of SPR peak angular
14
15 position shift (Figure S7), development of Z-average size over time (Figure S8), and
16
17 scattering-induced absorbance values in samples (Figure S9)
18
19

20 21 AUTHOR INFORMATION

22 23 Corresponding Authors

24
25 *E-mail: markus.selin@helsinki.fi

26
27 *E-mail: sami.nummelin@aalto.fi

28
29 *E-mail: luis.bimbo@strath.ac.uk

30 31 ORCID

32
33 Markus Selin: 0000-0002-4803-6606

34
35 Sami Nummelin: 0000-0003-2195-4818

36
37 Tapani Viitala: 0000-0001-9074-9450

38
39 Manu Lahtinen: 0000-0001-5561-3259

40
41 Luis M. Bimbo: 0000-0002-8876-8297
42
43
44
45
46

47 48 Notes

49
50 The authors declare no conflicts of interest.
51
52
53
54
55
56
57
58
59
60

ACKNOWLEDGMENTS

Financial support by the Academy of Finland (no. 276377 for L.M.B., no. 268616 for J.R. and no. 263504, 267497, and 273645 for M.A.K.), the Sigrid Jusélius Foundation, the Magnus Ehrnrooth Foundation, the Emil Aaltonen Foundation, the Finnish Cultural Foundation, Orion Research Foundation and Jane and Aatos Erkko Foundation is gratefully acknowledged. The work was carried out under the Academy of Finland's Centres of Excellence Programme (2014-2019).

REFERENCES

- (1) Müller, R. H.; Keck, C. M. Twenty Years of Drug Nanocrystals: Where Are We, and Where Do We Go? *Eur. J. Pharm. Biopharm.* **2012**, *80* (1), 1–3.
- (2) Rabinow, B. E. Nanosuspensions in Drug Delivery. *Nat. Rev. Drug Discov.* **2004**, *3* (9), 785–796.
- (3) Wu, L.; Zhang, J.; Watanabe, W. Physical and Chemical Stability of Drug Nanoparticles. *Adv. Drug Deliv. Rev.* **2011**, *63* (6), 456–469.
- (4) Nguyen, T. T. C.; Nguyen, C. K.; Nguyen, T. H.; Tran, N. Q. Highly Lipophilic Pluronic-Conjugated Polyamidoamine Dendrimer Nanocarriers as Potential Delivery System for Hydrophobic Drugs. *Mater. Sci. Eng. C* **2017**, *70* (2), 992–999.
- (5) Tuomela, A.; Hirvonen, J.; Peltonen, L. Stabilizing Agents for Drug Nanocrystals: Effect on Bioavailability. *Pharmaceutics* **2016**, *8* (2), 16.
- (6) Van Eerdenbrugh, B.; Stuyven, B.; Froyen, L.; Van Humbeeck, J.; Martens, J. A.; Augustijns, P.; Van den Mooter, G. Downscaling Drug Nanosuspension Production: Processing Aspects and Physicochemical Characterization. *AAPS Pharmscitech* **2009**, *10* (1), 44–53.
- (7) Peltonen, L.; Hirvonen, J. Pharmaceutical Nanocrystals by Nanomilling: Critical Process Parameters, Particle Fracturing and Stabilization Methods. *J. Pharm. Pharmacol.* **2010**, *62* (11), 1569–1579.
- (8) Bosman, A. W.; Janssen, H. M.; Meijer, E. W. About Dendrimers: Structure, Physical Properties, and Applications. *Chem. Rev.* **1999**, *99* (7), 1665–1688.
- (9) Caminade, A. M.; Laurent, R.; Majoral, J. P. Characterization of Dendrimers. *Adv.*

- 1
2
3 *Drug Deliv. Rev.* **2005**, *57* (15), 2130–2146.
- 4 (10) Tomalia, D. A.; Christensen, J. B.; Boas, U. *Dendrimers, Dendrons and Dendritic*
5 *Polymers*; Tomalia, D. A.; Christensen, J. B.; Boas, U., Ed.; Cambridge University
6 Press: New York, 2012.
- 7
8
9 (11) Sun, H.-J.; Zhang, S.; Percec, V. From Structure to Function via Complex
10 Supramolecular Dendrimer Systems. *Chem. Soc. Rev.* **2015**, *44* (12), 3900–3923.
- 11
12 (12) Tomalia, D. A. Dendrons/Dendrimers: Quantized, Nano-Element like Building Blocks
13 for Soft-Soft and Soft-Hard Nano-Compound Synthesis. *Soft Matter* **2010**, *6* (3), 456–
14 474.
- 15
16
17 (13) Khandare, J.; Calderón, M.; Dagia, N. M.; Haag, R. Multifunctional Dendritic
18 Polymers in Nanomedicine: Opportunities and Challenges. *Chem. Soc. Rev.* **2012**, *41*
19 (7), 2824–2848.
- 20
21
22 (14) Menjoge, A. R.; Kannan, R. M.; Tomalia, D. A. Dendrimer-Based Drug and Imaging
23 Conjugates: Design Considerations for Nanomedical Applications. *Drug Discov.*
24 *Today* **2010**, *15* (5–6), 171–185.
- 25
26
27 (15) Lee, C. C.; MacKay, J. A.; Fréchet, J. M. J.; Szoka, F. C. Designing Dendrimers for
28 Biological Applications. *Nat. Biotechnol.* **2005**, *23* (12), 1517–1526.
- 29
30 (16) Caminade, A.-M.; Laurent, R.; Delavaux-Nicot, B.; Majoral, J.-P. “Janus”
31 Dendrimers: Syntheses and Properties. *New J. Chem.* **2012**, *36* (2), 217–226.
- 32
33 (17) Percec, V.; Wilson, D. A.; Leowanawat, P.; Wilson, C. J.; Hughes, A. D.; Kaucher, M.
34 S.; Hammer, D. A.; Levine, D. H.; Kim, A. J.; Bates, F. S.; Davis, K. P.; Lodge, T. P.;
35 Klein, M. L.; DeVane, R. H.; Aqad, E.; Rosen, B. M.; Argintaru, A. O.; Sienkowska
36 M. J.; Rissanen, K.; Nummelin, S.; Ropponen, J. Self-Assembly of Janus Dendrimers
37 into Uniform Dendrimersomes and Other Complex Architectures. *Science*. **2010**, *328*
38 (5981), 1009–1014.
- 39
40
41 (18) Ropponen, J.; Nummelin, S.; Rissanen, K. Bisfunctionalized Janus Molecules. *Org.*
42 *Lett.* **2004**, *6* (15), 2495–2497.
- 43
44 (19) Tomalia, D. A.; Pulgam, V. R.; Swanson, D. R.; Huang, B. Janus Dendrimers and
45 Dendrons. U.S. Patent 7,977,452 B2, 2011.
- 46
47
48 (20) Nummelin, S.; Selin, M.; Legrand, S.; Ropponen, J.; Seitsonen, J.; Nykänen, A.;
49 Koivisto, J.; Hirvonen, J.; Kostiainen, M. A.; Bimbo, L. M. Modular Synthesis of Self-
50 Assembling Janus-Dendrimers and Facile Preparation of Drug-Loaded
51 Dendrimersomes. *Nanoscale* **2017**, *9* (21), 7189–7198.
- 52
53
54 (21) Filippi, M.; Patrucco, D.; Martinelli, J.; Botta, M.; Castro-Hartmann, P.; Tei, L.;

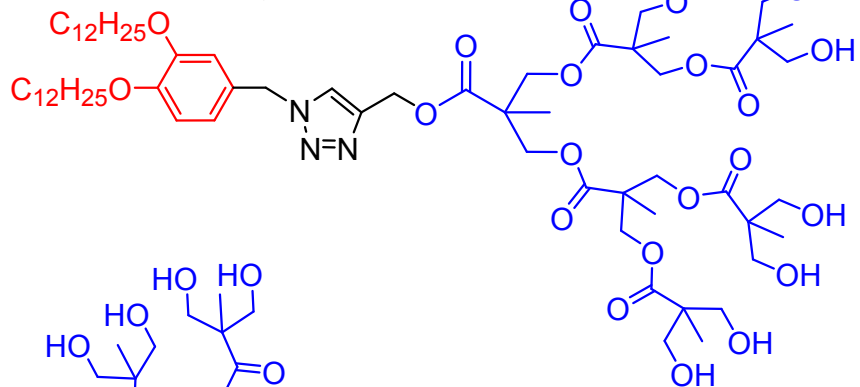
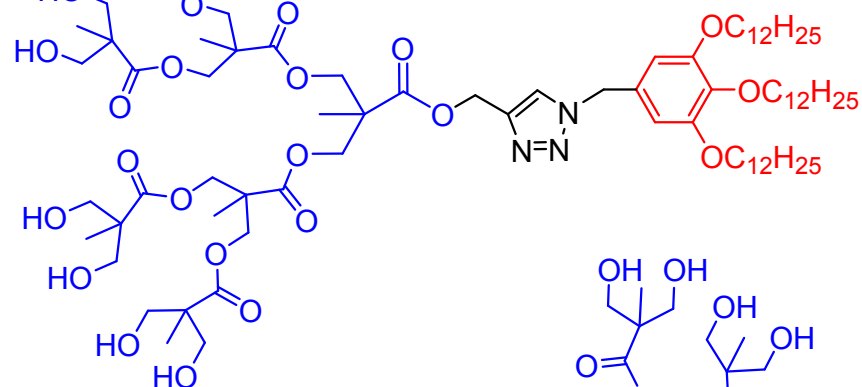
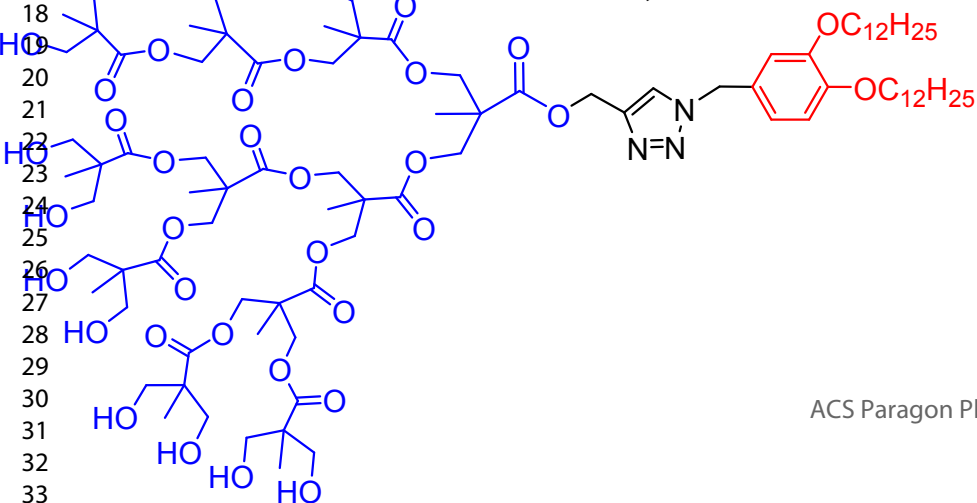
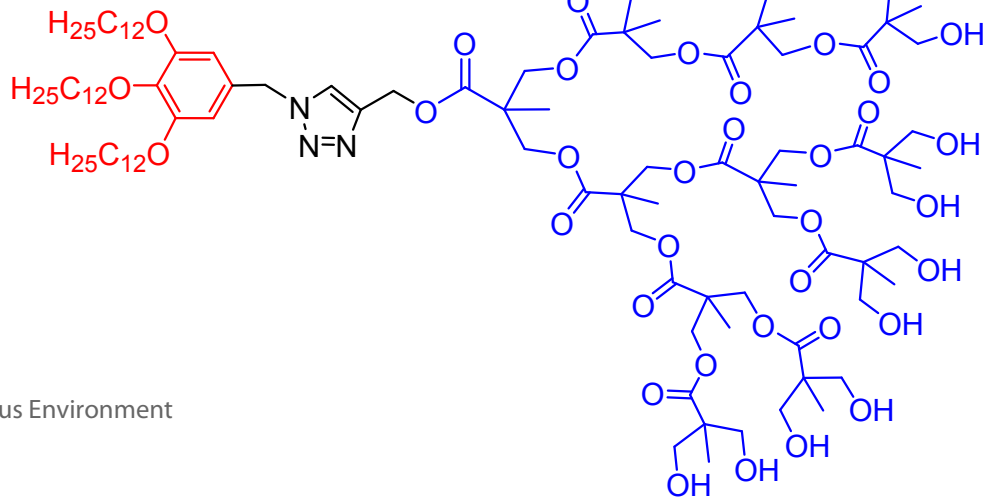
- 1
2
3 Terreno, E. Novel Stable Dendrimersome Formulation for Safe Bioimaging
4 Applications. *Nanoscale* **2015**, 7 (30), 12943–12954.
5
- 6 (22) Liu, X.; Zhou, J.; Yu, T.; Chen, C.; Cheng, Q.; Sengupta, K.; Huang, Y.; Li, H.; Liu,
7 C.; Wang, Y.; Posocco, P.; Wang, M.; Cui, Q.; Giorgio, S.; Fermeglia, M.; Qu, F.;
8 Pricl, S.; Liang, Z.; Rocchi, P.; Rossi, J. J.; Peng, L. Adaptive Amphiphilic Dendrimer-
9 Based Nanoassemblies as Robust and Versatile SiRNA Delivery Systems. *Angew.*
10 *Chem. Int. Ed.* **2014**, 53 (44), 11822–11827.
11
- 12 (23) Nazemi, A.; Gillies, E. R. Dendrimersomes with Photodegradable Membranes for
13 Triggered Release of Hydrophilic and Hydrophobic Cargo. *Chem. Commun.* **2014**, 50
14 (76), 11122–11125.
15
- 16 (24) Mikkilä, J.; Rosilo, H.; Nummelin, S.; Seitsonen, J.; Ruokolainen, J.; Kostianen, M.
17 A. Janus-Dendrimer-Mediated Formation of Crystalline Virus Assemblies. *ACS Macro*
18 *Lett.* **2013**, 2 (8), 720–724.
19
- 20 (25) Xiao, Q.; Zhang, S.; Wang, Z.; Sherman, S. E.; Moussodia, R.-O.; Peterca, M.;
21 Muncan, A.; Williams, D. R.; Hammer, D. A.; Vértesy, S.; Andre, S.; Gabius, H.-J.;
22 Klein, M. L.; Percec, V. Onion-like Glycodendrimersomes from Sequence-Defined
23 Janus Glycodendrimers and Influence of Architecture on Reactivity to a Lectin. *Proc.*
24 *Natl. Acad. Sci. U. S. A.* **2016**, 113 (5), 1162–1167.
25
- 26 (26) Zhang, S.; Xiao, Q.; Sherman, S. E.; Muncan, A.; Ramos Vicente, A. D. M.; Wang, Z.;
27 Hammer, D. A.; Williams, D.; Chen, Y.; Pochan, D. J.; Vertesy, S.; Andre, S.; Klein,
28 M. L.; Gabius, H.-J.; Percec, V. Glycodendrimersomes from Sequence-Defined Janus
29 Glycodendrimers Reveal High Activity and Sensor Capacity for the Agglutination by
30 Natural Variants of Human Lectins. *J. Am. Chem. Soc.* **2015**, 137 (41), 13334–13344.
31
- 32 (27) Zhang, S.; Moussodia, R.-O.; Sun, H.-J.; Leowanawat, P.; Muncan, A.; Nusbaum, C.
33 D.; Chelling, K. M.; Heiney, P. a.; Klein, M. L.; André, S.; Roy, R.; Gabius, H.-J.;
34 Percec, V. Mimicking Biological Membranes with Programmable Glycan Ligands
35 Self-Assembled from Amphiphilic Janus Glycodendrimers. *Angew. Chem. Int. Ed.*
36 **2014**, 53 (41), 10899–10903.
37
- 38 (28) Percec, V.; Leowanawat, P.; Sun, H. J.; Kulikov, O.; Nusbaum, C. D.; Tran, T. M.;
39 Bertin, A.; Wilson, D. A.; Peterca, M.; Zhang, S.; Kamat, N. P.; Vargo, K.; Moock, D.;
40 Johnston, E. D.; Hammer, D. A.; Pochan, D. J.; Chen, Y.; Chabre, Y. M.; Shiao, T. C.;
41 Bergeron-Brlek, M.; Andre, S.; Roy, R.; Gabius, H.-J.; Heiney, P. A. Modular
42 Synthesis of Amphiphilic Janus Glycodendrimers and Their Self-Assembly into
43 Glycodendrimersomes and Other Complex Architectures with Bioactivity to
44
45
46
47
48
49
50
51
52
53
54
55
56
57
58
59
60

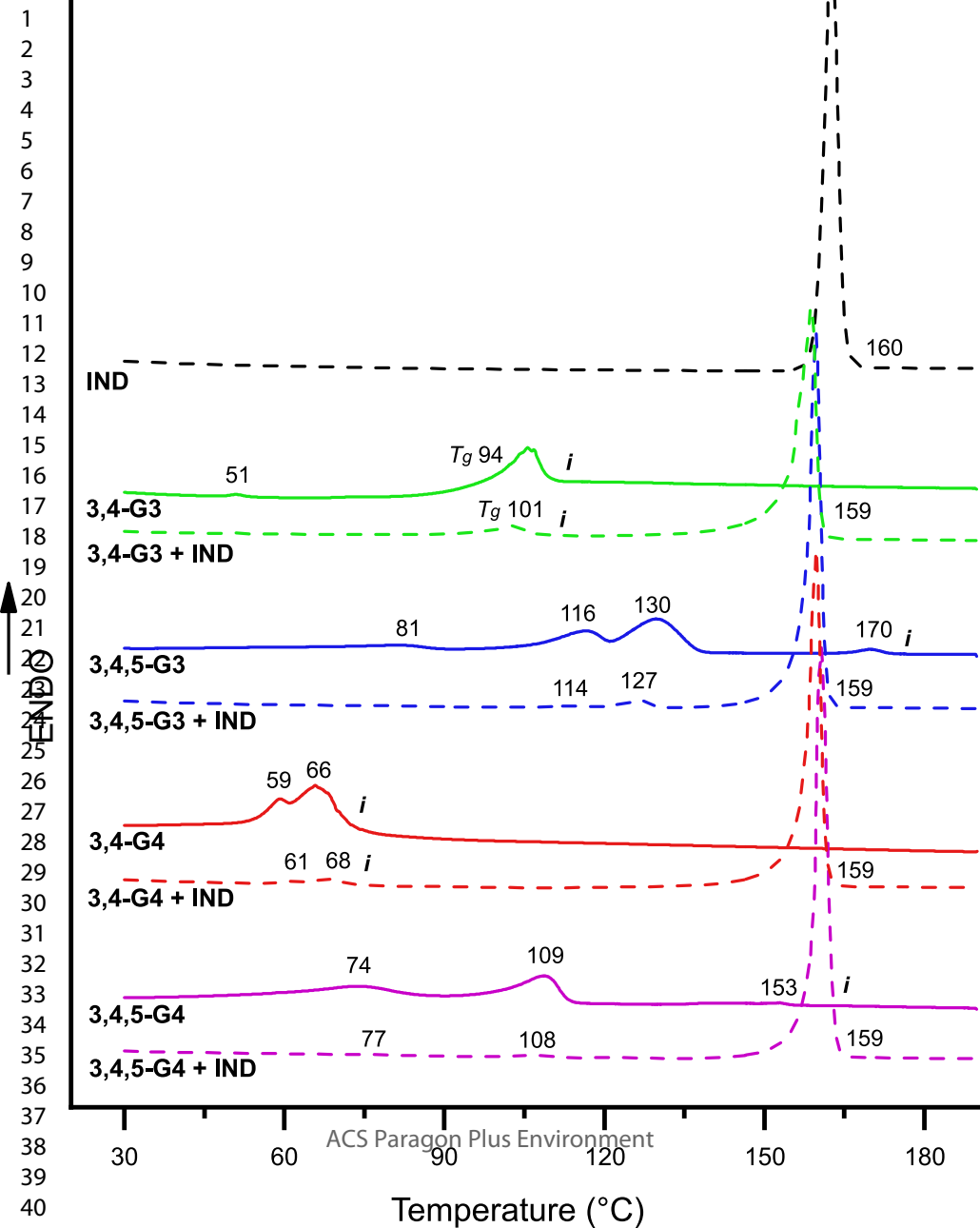
- 1
2
3 Biomedically Relevant Lectins. *J. Am. Chem. Soc.* **2013**, *135* (24), 9055–9077.
- 4 (29) Xiao, Q.; Rubien, J. D.; Wang, Z.; Reed, E. H.; Hammer, D. A.; Sahoo, D.; Heiney, P.
5 A.; Yadavalli, S. S.; Goulian, M.; Wilner, S. E.; Baumgart, T.; Vinogradov, S. A.;
6 Klein, M. L.; Percec, V. Self-Sorting and Coassembly of Fluorinated, Hydrogenated,
7 and Hybrid Janus Dendrimers into Dendrimersomes. *J. Am. Chem. Soc.* **2016**, *138*
8 (38), 12655–12663.
- 9 (30) Sherman, S. E.; Xiao, Q.; Percec, V. Mimicking Complex Biological Membranes and
10 Their Programmable Glycan Ligands with Dendrimersomes and
11 Glycodendrimersomes. *Chem. Rev.* **2017**, *117* (9), 6538–6631.
- 12 (31) Kopitz, J.; Xiao, Q.; Ludwig, A. K.; Romero, A.; Michalak, M.; Sherman, S. E.; Zhou,
13 X.; Dazen, C.; Vértesy, S.; Kaltner, H.; Klein, M. L.; Gabius, H.-J.; Percec, V.
14 Reaction of a Programmable Glycan Presentation of Glycodendrimersomes and Cells
15 with Engineered Human Lectins To Show the Sugar Functionality of the Cell Surface.
16 *Angew. Chem. Int. Ed.* **2017**, *56* (46), 14677–14681.
- 17 (32) Xiao, Q.; Yadavalli, S. S.; Zhang, S.; Sherman, S. E.; Fiorin, E.; da Silva, L.; Wilson,
18 D. A.; Hammer, D. A.; André, S.; Gabius, H.-J.; Klein, M. L.; Goulian, M.; Percec, V.
19 Bioactive Cell-like Hybrids Coassembled from (Glyco)Dendrimersomes with Bacterial
20 Membranes. *Proc. Natl. Acad. Sci. U. S. A.* **2016**, *113* (9), E1134–E1141.
- 21 (33) Xiao, Q.; Ludwig, A.-K.; Romanò, C.; Buzzacchera, I.; Sherman, S. E.; Vetro, M.;
22 Vértesy, S.; Kaltner, H.; Reed, E. H.; Möller, M.; Wilson, C. J.; Hammer, D. A.;
23 Oscarson, S.; Klein, M. L.; Gabius, H.-J.; Percec, V. Exploring Functional Pairing
24 between Surface Glycoconjugates and Human Galectins Using Programmable
25 Glycodendrimersomes. *Proc. Natl. Acad. Sci. U. S. A.* **2018**, *115* (11), E2509–E2518.
- 26 (34) Rosen, B. M.; Wilson, C. J.; Wilson, D. A.; Peterca, M.; Imam, M. R.; Percec, V.
27 Dendron-Mediated Self-Assembly, Disassembly, and Self-Organization of Complex
28 Systems. *Chem. Rev.* **2009**, *109* (11), 6275–6540.
- 29 (35) Xiao, Q.; Wang, Z.; Williams, D.; Leowanawat, P.; Peterca, M.; Sherman, S. E.;
30 Zhang, S.; Hammer, D. A.; Heiney, P. A.; King, S. R.; Markovitz, D. M.; Andre, S.;
31 Gabius, H.-J.; Klein, M. L.; Percec, V. Why Do Membranes of Some Unhealthy Cells
32 Adopt a Cubic Architecture? *ACS Cent. Sci.* **2016**, *2* (12), 943–953.
- 33 (36) Zhang, S.; Sun, H.-J.; Hughes, A. D.; Moussodia, R.-O.; Bertin, A.; Chen, Y.; Pochan,
34 D. J.; Heiney, P. A.; Klein, M. L.; Percec, V. Self-Assembly of Amphiphilic Janus
35 Dendrimers into Uniform Onion-like Dendrimersomes with Predictable Size and
36 Number of Bilayers. *Proc. Natl. Acad. Sci. U. S. A.* **2014**, *111* (25), 9058–9063.
- 37
38
39
40
41
42
43
44
45
46
47
48
49
50
51
52
53
54
55
56
57
58
59
60

- 1
2
3 (37) Zhang, S.; Sun, H. J.; Hughes, A. D.; Draghici, B.; Lejnieks, J.; Leowanawat, P.;
4 Bertin, A.; Otero De Leon, L.; Kulikov, O. V.; Chen, Y.; Pochan, D. J.; Heiney, P. A.;
5 Percec, V. "Single-Single" Amphiphilic Janus Dendrimers Self-Assemble into
6 Uniform Dendrimersomes with Predictable Size. *ACS Nano* **2014**, *8* (2), 1554–1565.
7
8
9 (38) Peterca, M.; Percec, V.; Leowanawat, P.; Bertin, A. Predicting the Size and Properties
10 of Dendrimersomes from the Lamellar Structure of Their Amphiphilic Janus
11 Dendrimers. *J. Am. Chem. Soc.* **2011**, *133* (50), 20507–20520.
12
13
14 (39) Röglin, L.; Lempens, E. H. M.; Meijer, E. W. A Synthetic "Tour de Force": Well-
15 Defined Multivalent and Multimodal Dendritic Structures for Biomedical
16 Applications. *Angew. Chem. Int. Ed.* **2011**, *50* (1), 102–112.
17
18
19 (40) Selin, M.; Peltonen, L.; Hirvonen, J.; Bimbo, L. M. Dendrimers and Their
20 Supramolecular Nanostructures for Biomedical Applications. *J. Drug Deliv. Sci.*
21 *Technol.* **2016**, *34*, 10-20.
22
23
24 (41) Auvinen, H.; Zhang, H.; Nonappa; Kopilow, A.; Niemelä, E. H.; Nummelin, S.;
25 Correia, A.; Santos, H. A.; Linko, V.; Kostianen, M. A. Protein Coating of DNA
26 Nanostructures for Enhanced Stability and Immunocompatibility. *Adv. Healthc. Mater.*
27 **2017**, *6* (18), 1700692.
28
29
30 (42) Meyers, S. R.; Juhn, F. S.; Griset, A. P.; Luman, N. R.; Grinstaff, M. W.; V. Anionic
31 Amphiphilic Dendrimers as Antibacterial Agents. *J. Am. Chem. Soc.* **2008**, *130* (44),
32 14444–14445.
33
34
35 (43) Ghobril, C.; Charoen, K.; Rodriguez, E. K.; Nazarian, A.; Grinstaff, M. W. A
36 Dendritic Thioester Hydrogel Based on Thiol-Thioester Exchange as a Dissolvable
37 Sealant System for Wound Closure. *Angew. Chem. Int. Ed.* **2013**, *52* (52), 14070–
38 14074.
39
40
41 (44) Nummelin, S.; Liljeström, V.; Saarikoski, E.; Ropponen, J.; Nykänen, A.; Linko, V.;
42 Seppälä, J.; Hirvonen, J.; Ikkala, O.; Bimbo, L. M.; Kostianen, M. A. Self-Assembly
43 of Amphiphilic Janus Dendrimers into Mechanically Robust Supramolecular
44 Hydrogels for Sustained Drug Release. *Chem. Eur. J.* **2015**, *21* (41), 14433–14439.
45
46
47 (45) Arseneault, M.; Wafer, C.; Morin, J.-F. Recent Advances in Click Chemistry Applied
48 to Dendrimer Synthesis. *Molecules* **2015**, *20* (5), 9263–9294.
49
50
51 (46) Wu, P.; Malkoch, M.; Hunt, J. N.; Vestberg, R.; Kaltgrad, E.; Finn, M. G.; Fokin, V.
52 V.; Sharpless, K. B.; Hawker, C. J. Multivalent, Bifunctional Dendrimers Prepared by
53 Click Chemistry. *Chem. Commun.* **2005**, *46*, 5775-5777.
54
55
56 (47) Liu, P.; Viitala, T.; Kartal-Hodzic, A.; Liang, H.; Laaksonen, T.; Hirvonen, J.;
57
58
59
60

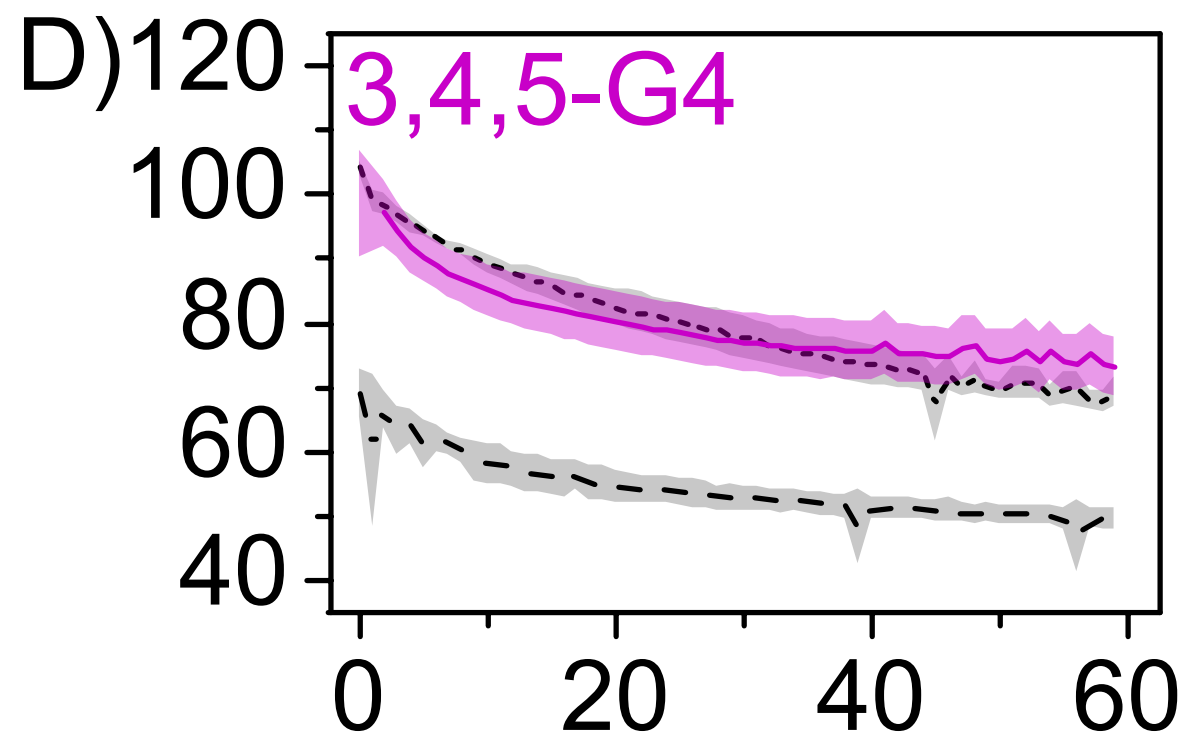
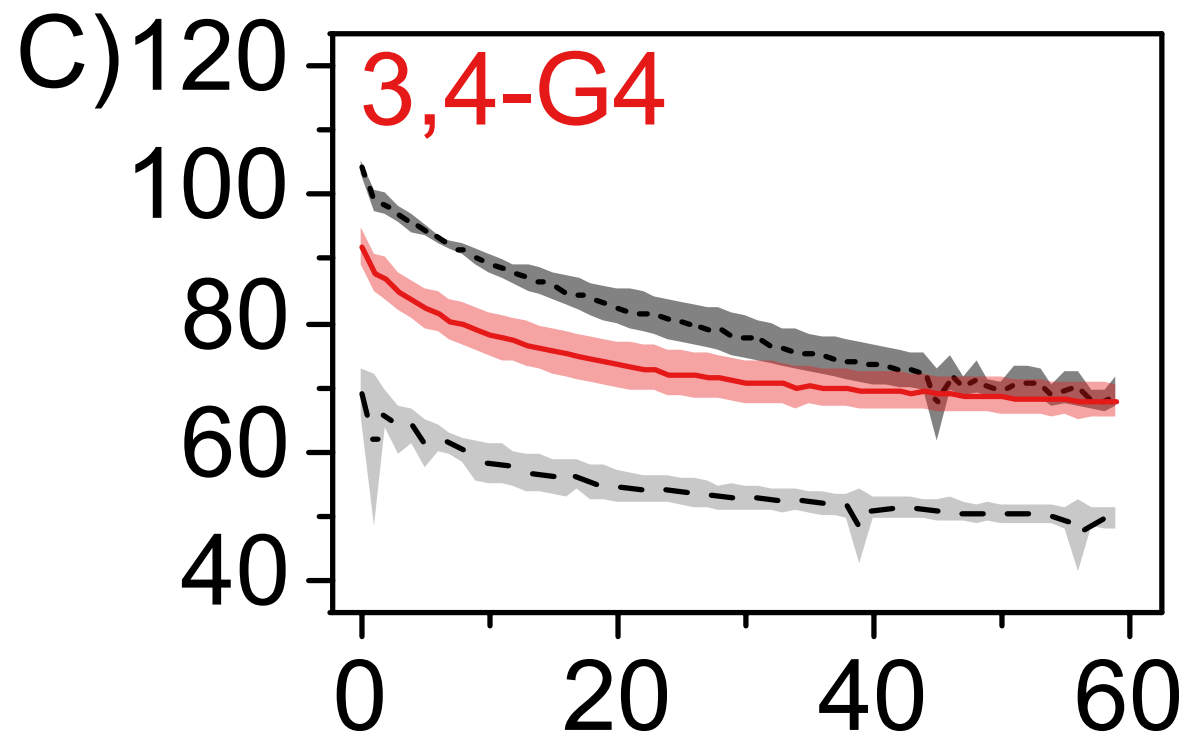
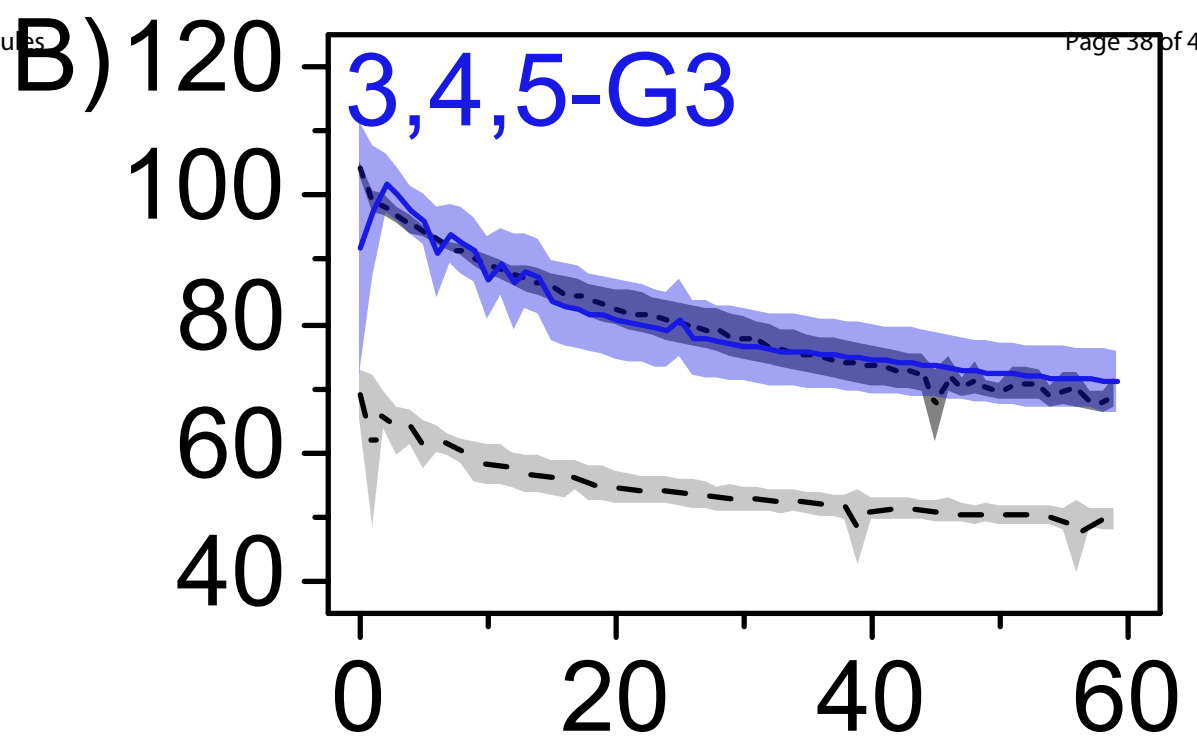
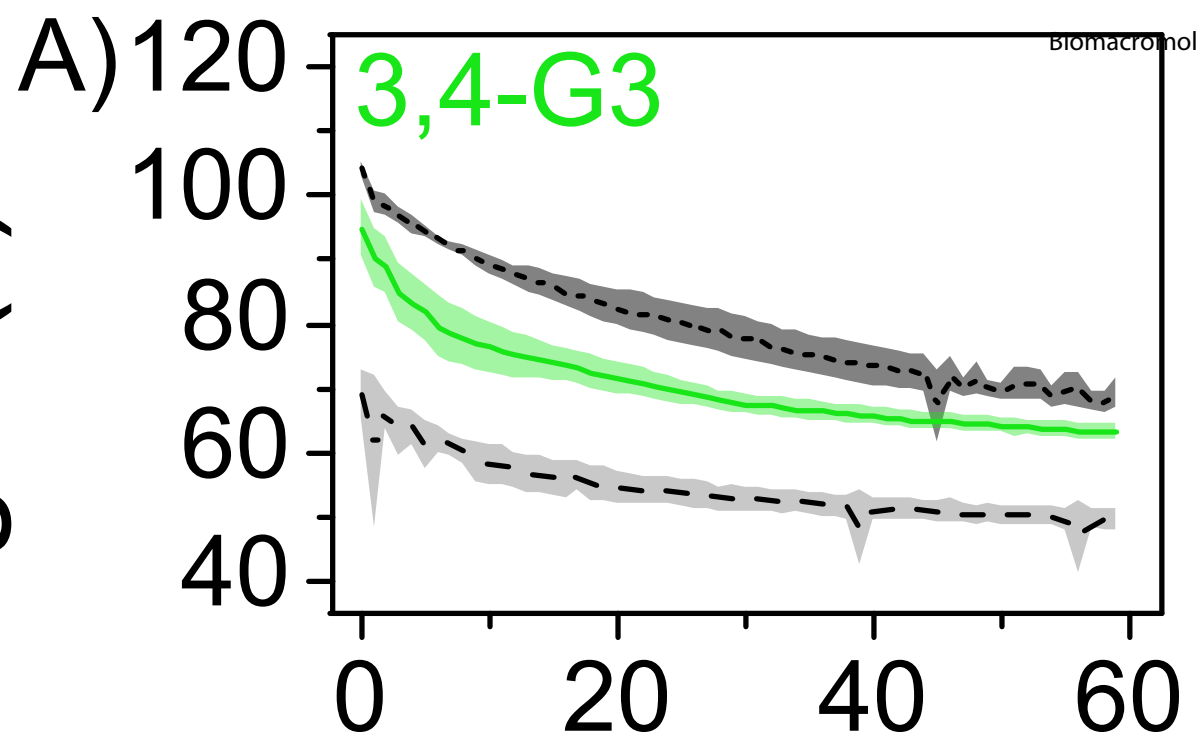
- 1
2
3 Peltonen, L. Interaction Studies between Indomethacin Nanocrystals and PEO/PPO
4 Copolymer Stabilizers. *Pharm. Res.* **2015**, *32* (2), 628–639.
- 5
6 (48) Van Eerdenbrugh, B.; Vermant, J.; Martens, J. A.; Froyen, L.; Van Humbeeck, J.;
7 Augustijns, P.; Van Den Mooter, G. A Screening Study of Surface Stabilization during
8 the Production of Drug Nanocrystals. *J. Pharm. Sci.* **2009**, *98* (6), 2091–2103.
- 9
10 (49) Liu, P.; Rong, X.; Laru, J.; Van Veen, B.; Kiesvaara, J.; Hirvonen, J.; Laaksonen, T.;
11 Peltonen, L. Nanosuspensions of Poorly Soluble Drugs: Preparation and Development
12 by Wet Milling. *Int. J. Pharm.* **2011**, *411* (1–2), 215–222.
- 13
14 (50) Surwase, S. A.; Boetker, J. P.; Saville, D.; Boyd, B. J.; Gordon, K. C.; Peltonen, L.;
15 Strachan, C. J. Indomethacin: New Polymorphs of an Old Drug. *Mol. Pharm.* **2013**, *10*
16 (12), 4472–4480.
- 17
18 (51) Chokshi, R. J.; Sandhu, H. K.; Iyer, R. M.; Shah, N. H.; Malick, A. W.; Zia, H.
19 Characterization of Physico-Mechanical Properties of Indomethacin and Polymers to
20 Assess Their Suitability for Hot-Melt Extrusion Processs as a Means to Manufacture
21 Solid Dispersion/Solution. *J. Pharm. Sci.* **2005**, *94* (11), 2463–2474.
- 22
23 (52) Bakatselou, V.; Oppenheim, R.C.; Dressman, J. B. Solubilization and Wetting Effects
24 of Bile Salts on the Dissolution of Steroids. *Pharm. Res.* **1991**, *8* (12), 1461–1469.
- 25
26 (53) Fox, H. W.; Zisman, W. A. The Spreading of Liquids on Low-Energy Surfaces. III.
27 Hydrocarbon Surfaces. *J. Colloid Sci.* **1952**, *7* (4), 428–442.
- 28
29 (54) Girifalco, L. A.; Good, R. J. A Theory for the Estimation of Surface and Interfacial
30 Energies. I. Derivation and Application to Interfacial Tension. *J. Phys. Chem.* **1957**, *61*
31 (7), 904–909.
- 32
33 (55) Sarnes, A.; Østergaard, J.; Jensen, S. S.; Aaltonen, J.; Rantanen, J.; Hirvonen, J.;
34 Peltonen, L. Dissolution Study of Nanocrystal Powders of a Poorly Soluble Drug by
35 UV Imaging and Channel Flow Methods. *Eur. J. Pharm. Sci.* **2013**, *50* (3–4), 511–519.
- 36
37 (56) Wassvik, C. M.; Holmén, A. G.; Bergström, C. A. S.; Zamora, I.; Artursson, P.
38 Contribution of Solid-State Properties to the Aqueous Solubility of Drugs. *Eur. J.*
39 *Pharm. Sci.* **2006**, *29* (3–4), 294–305.
- 40
41 (57) Inagi, T.; Muramatsu, T.; Nagai, H.; Terada, H. Mechanism of Indomethacin Partition
42 between N-Octanol and Water. *Chem. Pharm. Bull. (Tokyo)*. **1981**, *29* (8), 2330–2337.
- 43
44 (58) Najib, N.M.; Suleiman, M. S. The Effect of Hydrophilic Polymers and Surface Active
45 Agents on the Solubility of Indomethacin. *Int. J. Pharm.* **1985**, *24* (2–3), 165–171.
- 46
47 (59) Aceves-Hernandez, J. M.; Nicolás-Vázquez, I.; Aceves, F. J.; Hinojosa-Torres, J.; Paz,
48 M.; Castañ O, V. M. Indomethacin Polymorphs: Experimental and Conformational
49
50
51
52
53
54
55
56
57
58
59
60

- 1
2
3 Analysis. *J. Pharm. Sci.* **2009**, *98* (7), 2448–2463.
- 4 (60) Liu, P.; De Wulf, O.; Laru, J.; Heikkilä, T.; van Veen, B.; Kiesvaara, J.; Hirvonen, J.;
5 Peltonen, L.; Laaksonen, T. Dissolution Studies of Poorly Soluble Drug
6 Nanosuspensions in Non-Sink Conditions. *AAPS PharmSciTech* **2013**, *14* (2), 748–
7 756.
- 8
9
10
11 (61) Bisrat, Mikael; Nyström, C. Physicochemical Aspects of Drug Release. VIII. The
12 Relation between Particle Size and Surface Specific Dissolution Rate in Agitated
13 Suspensions. *Int. J. Pharm.* **1988**, *47* (1–3), 223–231.
- 14
15
16 (62) Keck, C. M.; Müller, R. H. Drug Nanocrystals of Poorly Soluble Drugs Produced by
17 High Pressure Homogenisation. *Eur. J. Pharm. Biopharm.* **2006**, *62* (1), 3–16.
- 18
19 (63) Simonelli, A. P.; Mehta, S. C.; Higuchi, W. I. Inhibition of Sulfathiazole Crystal
20 Growth by Polyvinylpyrrolidone. *J. Pharm. Sci.* **1970**, *59* (5), 633–638.
- 21
22 (64) Ricarte, R. G.; Li, Z.; Johnson, L. M.; Ting, J. M.; Reineke, T. M.; Bates, F. S.;
23 Hillmyer, M. A.; Lodge, T. P. Direct Observation of Nanostructures during Aqueous
24 Dissolution of Polymer/Drug Particles. *Macromolecules* **2017**, *50* (8), 3143–3152.
- 25
26
27
28
29
30
31
32
33
34
35
36
37
38
39
40
41
42
43
44
45
46
47
48
49
50
51
52
53
54
55
56
57
58
59
60

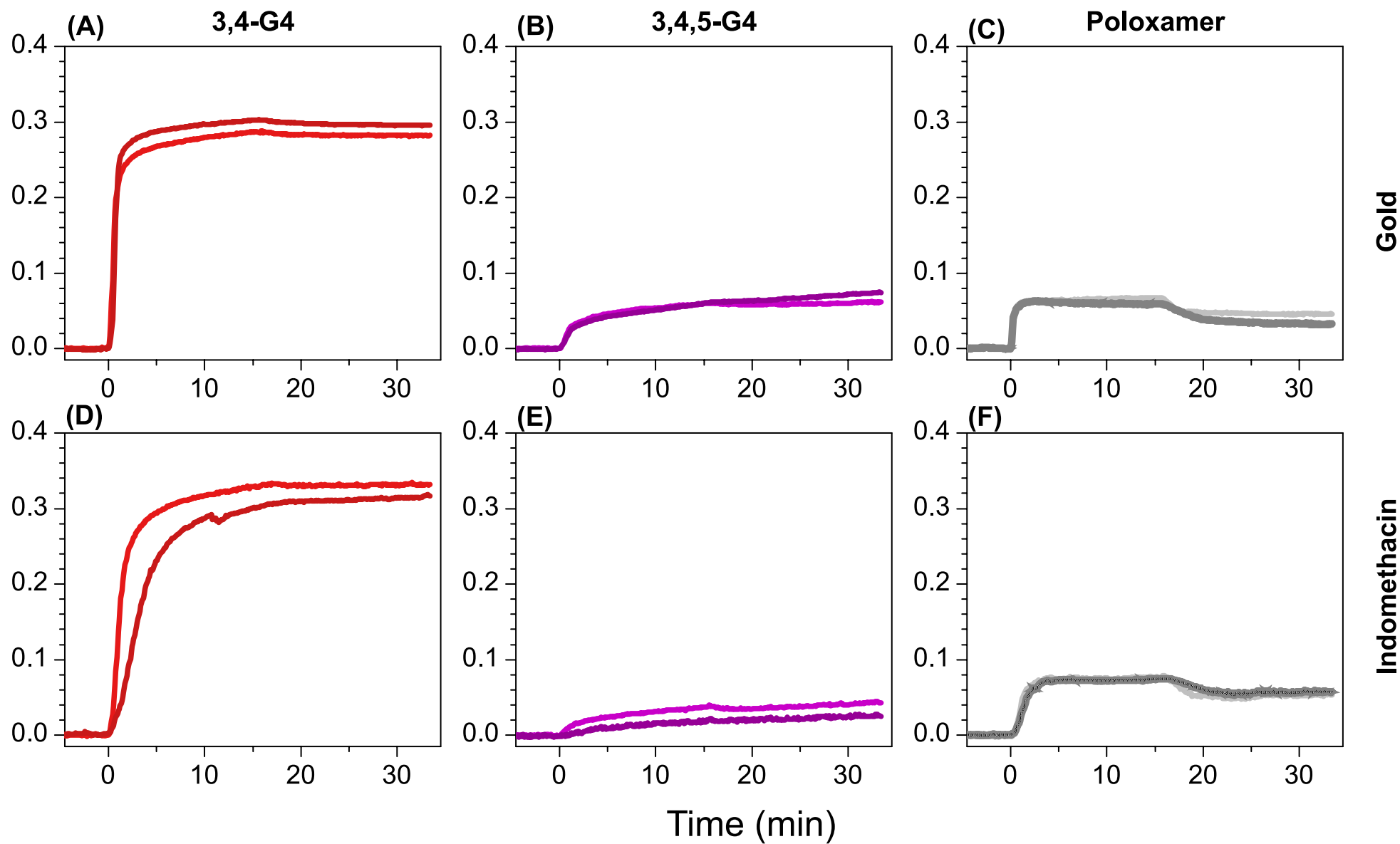
3,4-G3**3,4,5-G3****3,4-G4****3,4,5-G4**

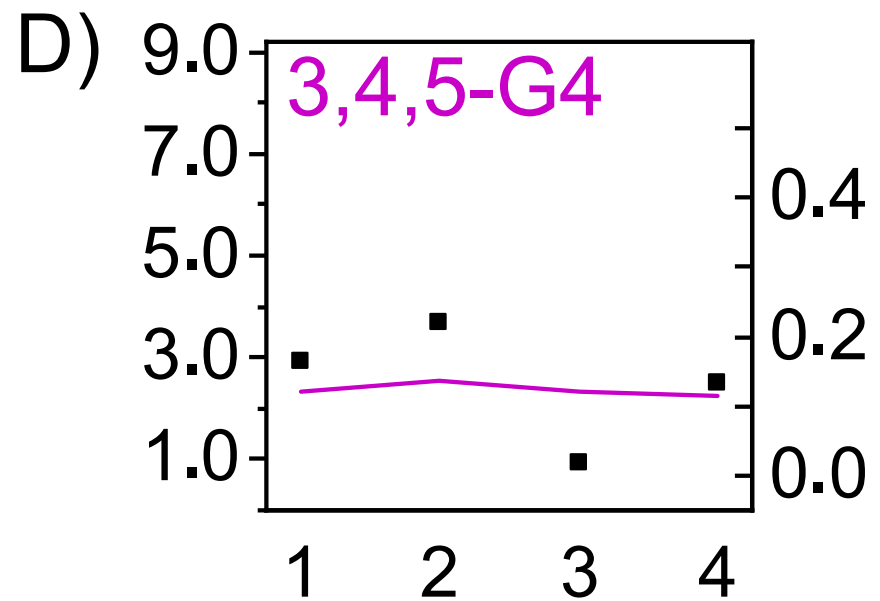
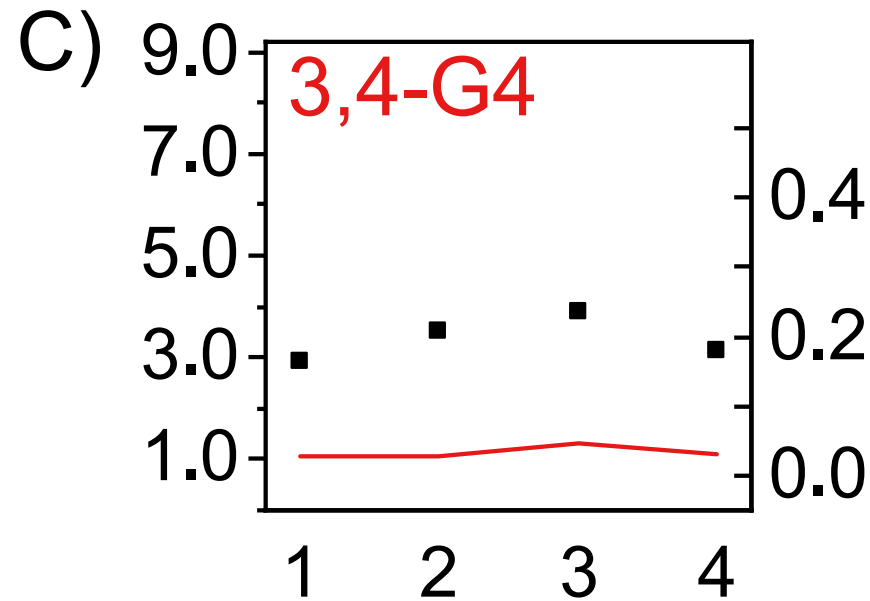
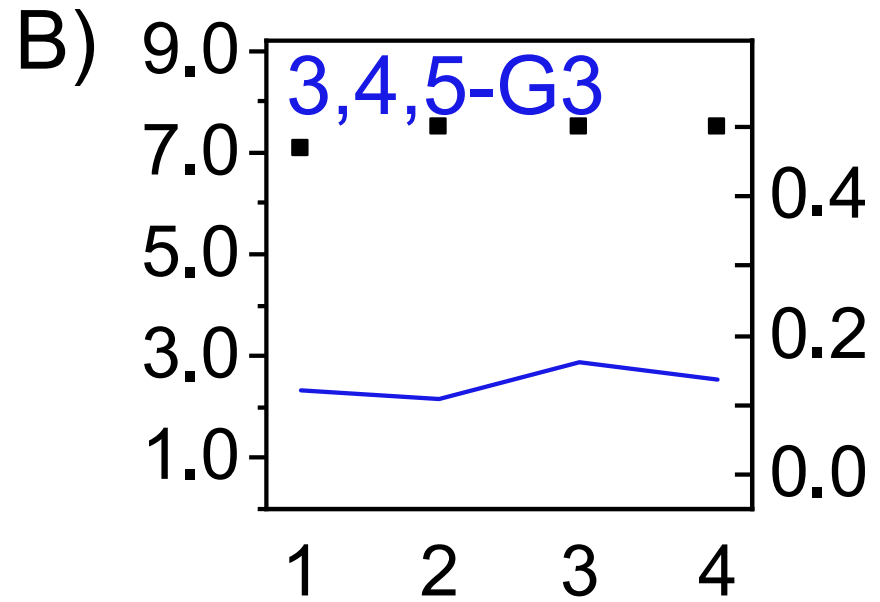
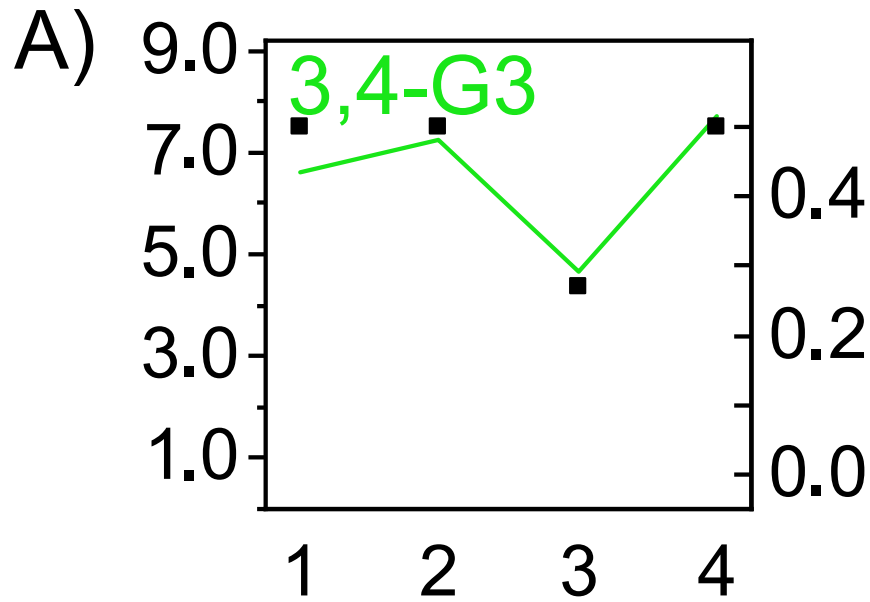


1
2
3
4
5
6
7
8
9
10
11
12
13
14
15
16
17
18
19
20
21
22
23
24
25
26
27
28
29
30
31
32
33
34
35
36
37
38
39
40
41
42
43
44
45
46
47
48
49
50
51
52
53



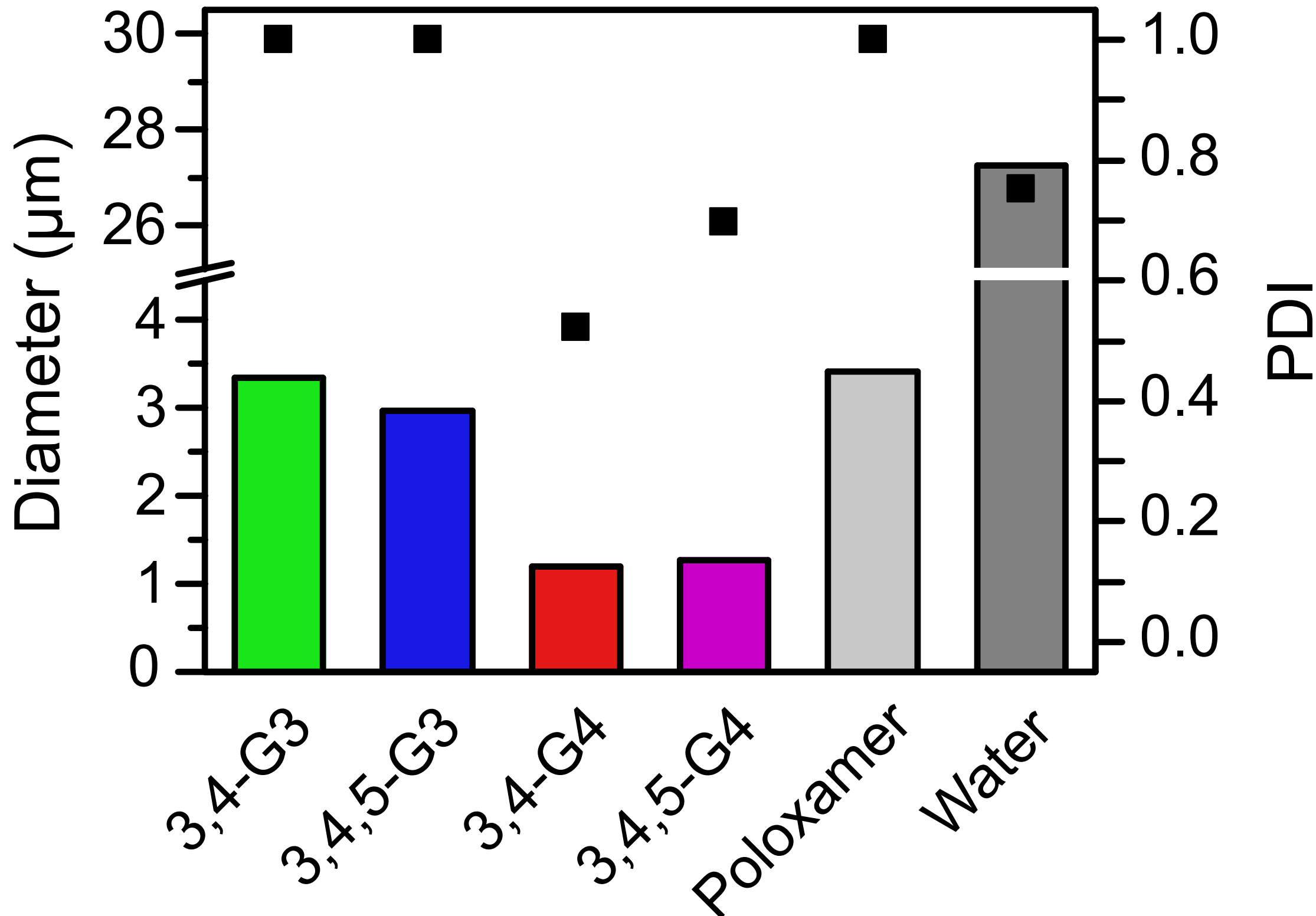
Time (s)

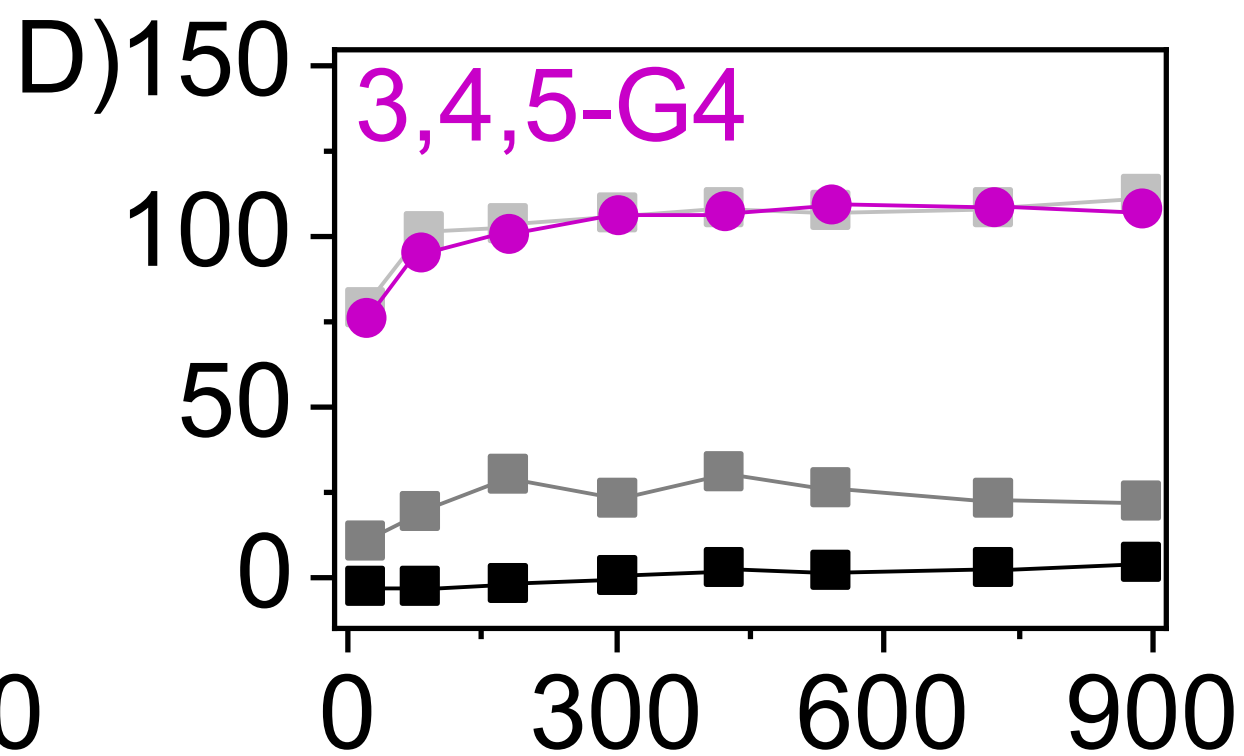
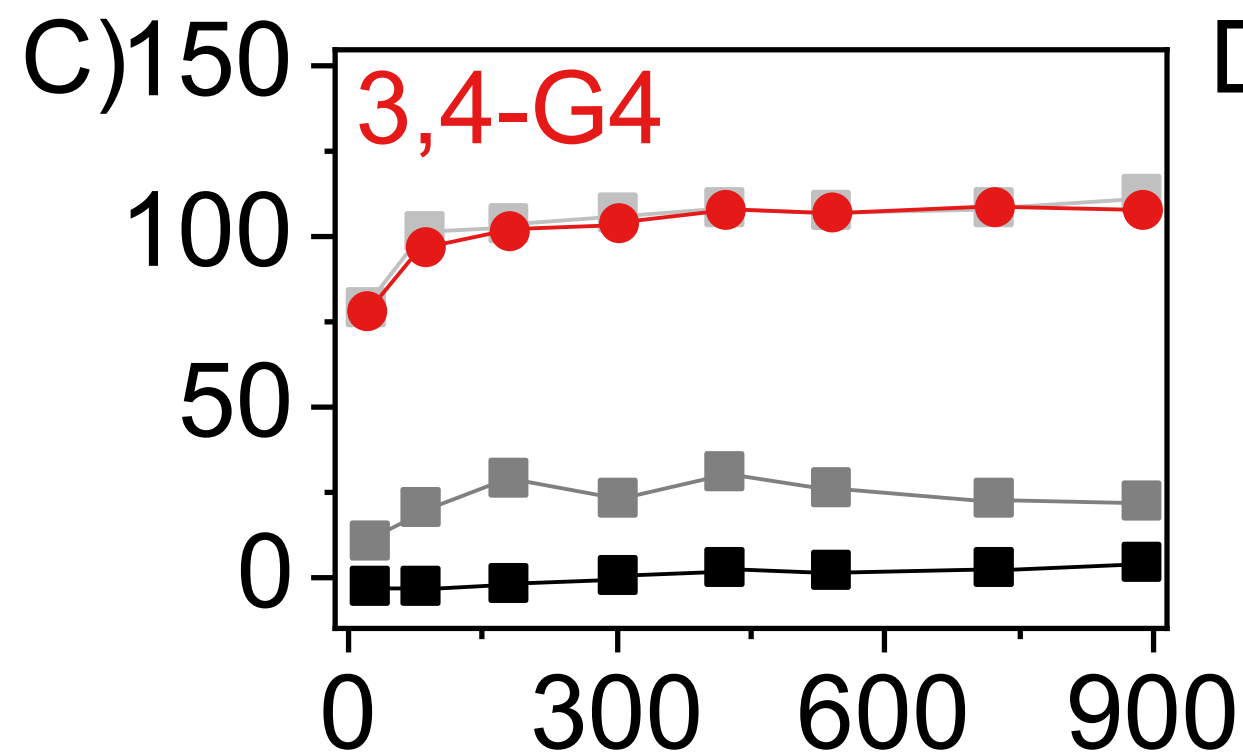
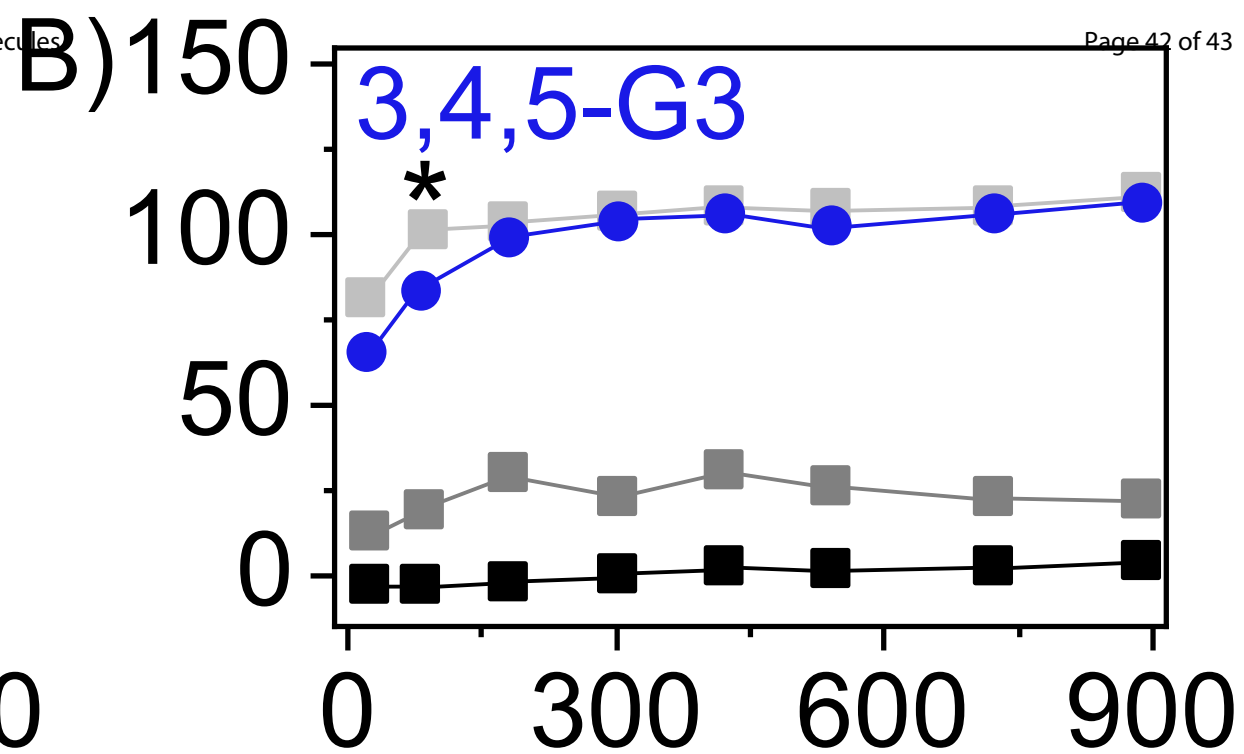
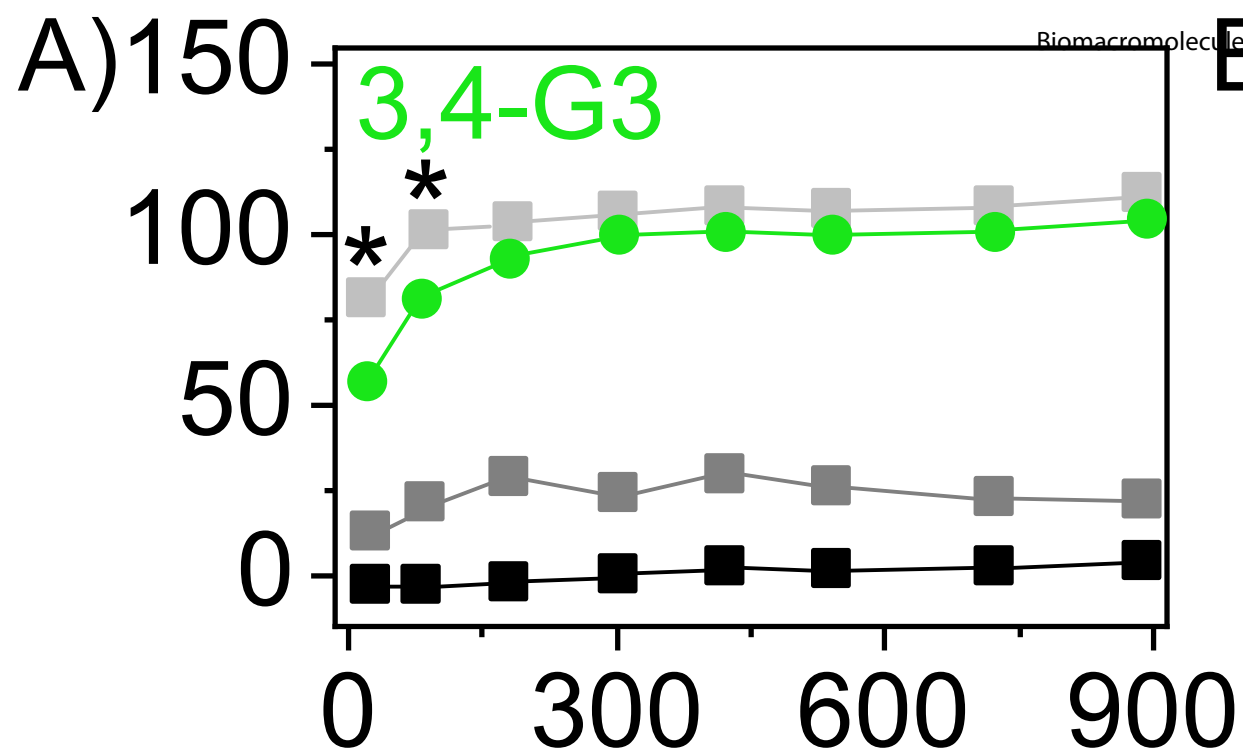
1
2
3
4
5
6
7
8
9
10
11
12
13
14
15
16
17
18
19
20
21
22
23
24
25
26
27
28
29
30
31
32
33
34
35
36
37
38
39
40
41
42
43
44
45
46
47

Diameter (μm)

PDI

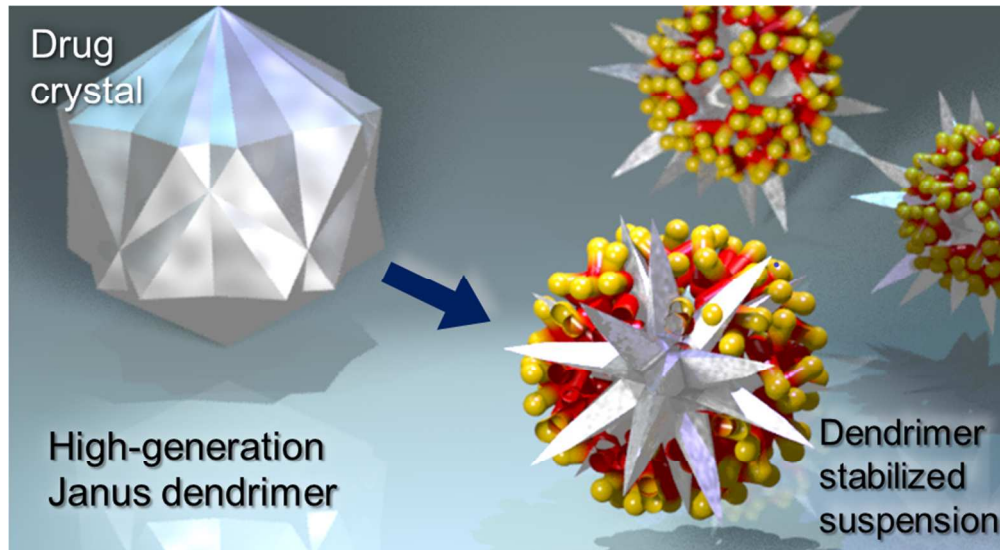
Time (weeks)





Time (s)

1
2
3
4
5
6
7
8
9
10
11
12
13
14
15
16
17
18
19
20
21
22
23
24
25
26
27
28
29
30
31
32
33
34
35
36
37
38
39
40
41
42
43
44
45
46
47
48
49
50
51
52
53



For Table of Contents Only

257x140mm (96 x 96 DPI)